by conventional $\alpha\beta$ TCR. The binding mode of 2C transgenic TCR was investigated using an IgG1-H2K^b dimer, and evidence for TCR $\alpha\beta$ dimerization was obtained by data deconvolution. To confirm the cooperative engagement of glycolipid Ag, we also used IgG1-CD1d1 and IgG1-H2K^b dimer similar to that used to investigate the 2C TCR (50). The results supported cooperative Ag engagement by iNKT cell, but not CTL receptors. Thus, the relationship of our findings with those previously reported is unclear.

Because H2K^b and CD1d1 tetramers were built upon the same batches of streptavidin-PE/allophycocyanin, cooperativity in one and not the other precludes conformational change in streptavidin or the fluorochrome. Furthermore, because of the wide separation between monomeric subunits of tetrameric CD1d1, it is extremely unlikely that a conformational change within CD1d1 itself is responsible for the observed Hill coefficient. This is further emphasized by the fact that CD1d1 dimers made in a manner distinct from tetramers also show cooperative binding. Cooperativity is independent of the parameters of glycolipid binding to CD1d1, because OCH, which interacts with CD1d1 with differing properties than αGalCer, had essentially the same Hill coefficient as αGalCer. Thus, the change in Hill coefficient does not reflect a change in the structure of CD1d1 tetramer, but rather a different organization and/or orientation of the TCR engaging such Ags.

How iNKT cells respond to self-Ag and yet remain quiescent in physiological situations remains unclear. In this study, we demonstrate that iNKT cell receptors exhibit cooperative engagement of glycolipid Ag. Cooperativity in biological systems is a common mechanism for achieving sensitivity to relatively modest changes in the strength of the signal (33, 63). In other words, a relatively small change in ligand concentration will result in full binding/activation of an enzyme/receptor. It is possible that iNKT cells use cooperativity to induce sensitive response to a small change in the concentration of self-Ag. In support of this hypothesis, self-Ag recognition of ex vivo-isolated iNKT cells is dependent on high levels of CD1d1 expression by target cells (2), and conversely, iNKT cell hybridomas recognizing physiologic levels of CD1d1 on target thymocytes or dendritic cells have high levels of Va14Ja18 TCR expression (6). Thus, the finding of cooperativity in iNKT cell Ag engagement, but not among CTL recognizing peptidic Ags may be one mechanism by which iNKT cells recognize self-Ag(s).

Our data indicate that the structure and/or organization of the iNKT cell receptor may be distinct from $\alpha\beta$ TCR of CTL. FG loop within the Cb domain is a large, evolutionarily conserved structure, which forms a wall at the region where Cb and Vb domains of the TCR β-chain join to form a cavity (77). Ab mapping studies revealed that the FG loop is in close proximity to one of the CD3ϵ subunits (78). Transgenic mice expressing the TCR β-chain mutant lacking the FG loop have no gross deficiencies in the development and function of conventional CD4 and CD8 T cells (79), implying that $\alpha\beta$ TCR pairing and surface expression are not grossly impaired. However, a careful analysis in a single specificity TCR transgenic system revealed that thymocytes lacking the FG loop had impaired negative selection (80), but TCR $\alpha\beta$ pairing and expression were unhindered. In contrast, however, Va14Ja18 TCR α-chain was found not to pair at all with a Vb8.2-FG loop mutant, and hence, the mutant mice were impaired in iNKT cell development (81). Interestingly, the anti-TCRβ Ab H57-597, which exhibits strong FRET in conjunction with the CD1d1-αGalCer tetramer specifically binds the FG loop (77, 79). However, FRET was not observed in conjunction with H2K^b tetramers or dimers. FRET is observed between CD8a of 2C-transgenic CTL and H2K^b, suggesting the engagement of CD8a by monomeric H2K^b (82). Taken together, the data strongly suggest that the structure and/or the organization of the Va14Ja18 TCR complex are distinct from $\alpha\beta$ TCR of conventional T cells, which might potentially account for the cooperative engagement of glycolipid Ags.

In conclusion, our findings demonstrate that iNKT cell functions are controlled by narrow avidity thresholds for glycolipid Ags and demonstrate novel properties of their Ag receptor that may have an important role in iNKT cell activation. These findings have important implications for the therapeutic use of iNKT cells.

Acknowledgments

We are greatly indebted to D. H. Margulies, D. Kranz, and S. Jameson for critical evaluation of the binding data and helpful comments on the manuscript, as well as to S. Roopenian for generous supplies of CTL clones. We thank M. Stanic for assistance and expertise in Hill constant determinations. We thank M. Wilson for CFSE labeling and in vitro expansion protocols. We thank Kirin Brewery for synthetic αGalCer; M. Taniguchi for B6-*Ja18*$^{-/-}$ mice; A. Bendelac and K. Hayakawa for NKT hybridomas; O. Naidenko and M. Kronenberg for helpful protocols for CD1 tetramer preparation; and A. J. Joyce for technical assistance.

References

1. Joyce, S. 2001. CD1d and natural T cells: how their properties jump start the immune system. *Cell. Mol. Life Sci. 58:442.*
2. Bendelac, A., O. Lantz, M. E. Quimby, J. W. Yewdell, J. R. Bennink, and R. R. Brutkiewicz. 1995. CD1 recognition of mouse NK1$^+$ T lymphocytes. *Science 268:863.*
3. Brossay, L., S. Tangri, M. Bix, S. Cardell, R. Locksley, and M. Kronenberg. 1998. Mouse CD1-autoreactive T cells have diverse patterns of reactivity to CD1$^+$ targets. *J. Immunol. 160:3681.*
4. Chiu, Y. H., J. Jayawardena, A. Weiss, D. Lee, S. H. Park, A. Dautry-Varsat, and A. Bendelac. 1999. Distinct subsets of CD1d-restricted T cells recognize self-antigens loaded in different cellular compartments. *J. Exp. Med. 189:103.*
5. Molano, A., S. H. Park, Y. H. Chiu, S. Nosseir, A. Bendelac, and M. Tsuji. 2000. The IgG response to the circumsporozoite protein is MHC class II-dependent and CD1d-independent: exploring the role of GPIs in NK T cell activation and antimalarial responses. *J. Immunol. 164:5005.*
6. Park, S.-H., J. H. Roark, and A. Bendelac. 1998. Tissue-specific recognition of mouse CD1 molecules. *J. Immunol. 160:3128.*
7. Chiu, Y. H., S. H. Park, K. Benlagha, C. Forestier, J. Jayawardena-Wolf, P. B. Savage, L. Teyton, and A. Bendelac. 2002. Multiple defects in antigen presentation and T cell development by mice expressing cytoplasmic tail-truncated CD1d. *Nat. Immunol. 3:55.*
8. De Silva, A. D., J.-J. Park, N. Matsuki, A. K. Stanic, R. R. Brutkiewicz, M. E. Medof, and S. Joyce. 2002. Lipid protein interactions: the assembly of CD1d1 with cellular phospholipids occurs in the endoplasmic reticulum. *J. Immunol. 168:723.*
9. Roberts, T. J., V. Sriram, P. M. Spence, M. Gui, K. Hayakawa, I. Bacik, J. R. Bennink, J. W. Yewdell, and R. R. Brutkiewicz. 2002. Recycling CD1d1 molecules present endogenous antigens processed in an endocytic compartment to NKT cells. *J. Immunol. 168:5409.*
10. Brossay, L., M. Chioda, N. Burdin, Y. Koezuka, G. Casorati, P. Dellabona, and M. Kronenberg. 1998. CD1d-mediated recognition of an α-galactosylceramide by natural killer T cells is highly conserved through mammalian evolution. *J. Exp. Med. 188:1521.*
11. Burdin, N., L. Brossay, Y. Koezuka, S. T. Smiley, M. J. Grusby, M. Gui, M. Taniguchi, K. Hayakawa, and M. Kronenberg. 1998. Selective ability of mouse CD1 to present glycolipids: α-galactosylceramide specifically stimulates Vα14$^+$ NK T lymphocytes. *J. Immunol. 161:3271.*
12. Kawano, T., J. Cui, Y. Koezuka, I. Toura, Y. Kaneko, K. Motoki, H. Ueno, R. Nakagawa, H. Sato, E. Kondo, et al. 1997. CD1d-restricted and TCR-mediated activation of Vα14 NKT cells by glycosylceramides. *Science 278:1626.*
13. Nieda, M., A. Nicol, Y. Koezuka, A. Kikuchi, T. Takahashi, H. Nakamura, H. Furukawa, T. Yabe, Y. Ishikawa, K. Tadokoro, and T. Juji. 1999. Activation of human Vα24NKT cells by α-glycosylceramide in a CD1d-restricted and Vα24TCR-mediated manner. *Hum. Immunol. 60:10.*
14. Spada, F. M., Y. Koezuka, and S. A. Porcelli. 1998. CD1d-restricted recognition of synthetic glycolipid antigens by human natural killer T cells. *J. Exp. Med. 188:1529.*
15. Stanic, A. K., A. D. De Silva, J. J. Park, V. Sriram, S. Ichikawa, Y. Hirabyashi, K. Hayakawa, L. Van Kaer, R. R. Brutkiewicz, and S. Joyce. 2003. Defective presentation of the CD1d1-restricted natural Va14Ja18 NKT lymphocyte antigen caused by β-D-glucosylceramide synthase deficiency. *Proc. Natl. Acad. Sci. USA 100:1849.*
16. Bendelac, A., and R. Medzhitov. 2002. Adjuvants of immunity: harnessing innate immunity to promote adaptive immunity. *J. Exp. Med. 195:F19.*
17. Hong, S., M. T. Wilson, I. Serizawa, L. Wu, N. Singh, O. V. Naidenko, T. Miura, T. Haba, D. C. Scherer, J. Wei, et al. 2001. The natural killer T-cell ligand α-galactosylceramide prevents autoimmune diabetes in non-obese diabetic mice. *Nat. Med. 7:1052.*

18. Sharif, S., G. A. Arreaza, P. Zucker, Q. S. Mi, J. Sondhi, O. V. Naidenko, M. Kronenberg, Y. Koezuka, T. L. Delovitch, J. M. Gombert, et al. 2001. Activation of natural killer T cells by α-galactosylceramide treatment prevents the onset and recurrence of autoimmune type 1 diabetes. *Nat. Med. 7:1057.*
19. Miyamoto, K., S. Miyake, and T. Yamamura. 2001. A synthetic glycolipid prevents autoimmune encephalomyelitis by inducing Th2 bias of natural killer T cells. *Nature 413:531.*
20. Singh, A. K., M. T. Wilson, S. Hong, D. Olivares-Villagomez, C. Du, A. K. Stanic, S. Joyce, S. Sriram, Y. Koezuka, and L. Van Kaer. 2001. Natural killer T cell activation protects mice against experimental autoimmune encephalomyelitis. *J. Exp. Med. 194:1801.*
21. Wilson, M. T., A. K. Singh, and L. Van Kaer. 2002. Immunotherapy with ligands of natural killer T cells. *Trends Mol. Med. 8:225.*
22. Margulies, D. H. 1997. Interactions of TCRs with MHC-peptide complexes: a quantitative basis for mechanistic models. *Curr. Opin. Immunol. 9:390.*
23. Davis, M. M., J. J. Boniface, Z. Reich, D. Lyons, J. Hampl, B. Arden, and Y. Chien. 1998. Ligand recognition by αβ T cell receptors. *Annu. Rev. Immunol. 16:523.*
24. Germain, R. N., and I. Stefanova. 1999. The dynamics of T cell receptor signaling: complex orchestration and the key roles of tempo and cooperation. *Annu. Rev. Immunol. 17:467.*
25. Garcia, K. C., L. Teyton, and I. A. Wilson. 1999. Structural basis for T cell recognition. *Annu. Rev. Immunol. 17:369.*
26. Sidobre, S., O. V. Naidenko, B. C. Sim, N. R. Gascoigne, K. C. Garcia, and M. Kronenberg. 2002. The Vα14 NKT cell TCR exhibits high-affinity binding to a glycolipid/CD1d complex. *J. Immunol. 169:1340.*
27. Schumann, J., R. B. Voyle, B. Y. Wei, and H. R. MacDonald. 2003. Influence of the TCR Vβ domain on the avidity of CD1d:α-galactosylceramide binding by invariant Vα14 NKT cells. *J. Immunol. 170:5815.*
28. Kalergis, A. M., N. Boucheron, M. A. Doucey, E. Palmieri, E. C. Goyarts, Z. Vegh, I. F. Luescher, and S. G. Nathenson. 2001. Efficient T cell activation requires an optimal dwell-time of interaction between the TCR and the pMHC complex. *Nat. Immunol. 2:229.*
29. Holler, P. D., and D. M. Kranz. 2003. Quantitative analysis of the contribution of TCR/pepMHC affinity and CD8 to T cell activation. *Immunity 18:255.*
30. Garcia, K. C., C. A. Scott, A. Brunmark, F. R. Carbone, P. A. Peterson, I. A. Wilson, and L. Teyton. 1996. CD8 enhances formation of stable T-cell receptor/MHC class I molecule complexes. *Nature 384:577.*
31. Luescher, I. F., E. Vivier, A. Layer, J. Mahiou, F. Godeau, B. Malissen, and P. Romero. 1995. CD8 modulation of T-cell antigen receptor-ligand interactions on living cytotoxic T lymphocytes. *Nature 373:353.*
32. Jelonek, M. T., B. J. Classon, P. J. Hudson, and D. H. Margulies. 1998. Direct binding of the MHC class I molecule H-2L^d to CD8: interaction with the amino terminus of a mature cell surface protein. *J. Immunol. 160:2809.*
33. Germain, R. N. 2001. The art of the probable: system control in the adaptive immune system. *Science 293:240.*
34. Fersht, A. 1999. *Structure and Mechanism in Protein Science.* Freeman, New York.
35. Benlagha, K., A. Weiss, A. Beavis, L. Teyton, and A. Bendelac. 2000. In vivo identification of glycolipid antigen-specific T cells using fluorescent CD1d tetramers. *J. Exp. Med. 191:1895.*
36. Cui, J., S. Tahiro, T. Kawano, H. Sato, E. Kondo, I. Toura, Y. Kaneko, H. Koseki, M. Kanno, and M. Taniguchi. 1997. Requirement for Vα14 NKT cells in IL-12-mediated rejection of tumors. *Science 278:1623.*
37. Mendiratta, S. K., W. D. Martin, S. Hong, A. Boesteanu, S. Joyce, and L. Van Kaer. 1997. *CD1d1* mutant mice are deficient in natural T cells that promptly produce IL-4. *Immunity 6:469.*
38. Choi, E. Y., Y. Yoshimura, G. J. Christianson, T. J. Sproule, S. Malarkannan, N. Shastri, S. Joyce, and D. C. Roopenian. 2001. Quantitative analysis of the immune response to mouse non-MHC transplantation antigens in vivo: the H60 histocompatibility antigen dominates over all others. *J. Immunol. 166:4370.*
39. Mylin, L. M., T. D. Schell, D. Roberts, M. Epler, A. Boesteanu, E. J. Collins, J. A. Frelinger, S. Joyce, and S. S. Tevethia. 2000. Quantitation of CD8$^+$ T-lymphocyte responses to multiple epitopes from Simian virus 40 (SV40) large T antigen in C57BL/6 mice immunized with SV40, SV40 T-antigen-transformed cells, or vaccinia virus recombinants expressing full-length T antigen or epitope minigenes. *J. Virol. 74:6922.*
40. Gui, M., J. Li, L. J. Wen, R. R. Hardy, and K. Hayakawa. 2001. TCRβ chain influences but does not solely control autoreactivity of Vα14Jα281 T cells. *J. Immunol. 167:6239.*
41. Lantz, O., and A. Bendelac. 1994. An invariant T cell receptor α chain is used by a unique subset of MHC class I specific CD4$^+$ and CD4$^-$8$^-$ T cells in mice and humans. *J. Exp. Med. 180:1097.*
42. Limbird, L. E. 1996. *Cell Surface Receptors: A Short Course on Theory and Methods.* Kluwer, Boston.
43. Matsuki, N., A. K. Stanic, M. E. Embers, L. Van Kaer, L. Morel, and S. Joyce. 2003. Genetic dissection of Va14Ja18 natural T cell number and function in autoimmune-prone mice. *J. Immunol. 170:5429.*
44. Joyce, S., A. S. Woods, J. W. Yewdell, J. R. Bennink, A. D. De Silva, A. Boesteanu, S. P. Balk, R. J. Cotter, and R. R. Brutkiewciz. 1998. Natural ligand of mouse CD1d1: cellular glycosylphosphatidylinositol. *Science 279:1541.*
45. Boyd, L. F., S. Kozlowski, and D. H. Margulies. 1992. Solution binding of an antigenic peptide to a major histocompatibility complex class I molecule and the role of β_2-microglobulin. *Proc. Natl. Acad. Sci. USA 89:2242.*
46. Corr, M., A. E. Slanetz, L. F. Boyd, M. T. Jelonek, S. Khilko, B. K. AlRamadi, Y. S. Kim, S. E. Maher, A. L. M. Bothwell, and D. H. Margulies. 1994. T cell receptor-MHC class I peptide interactions: affinity, kinetics and specificity. *Science 265:946.*
47. Matsui, K., J. J. Boniface, P. A. Reay, H. Schild, B. Fazekas de St. Groth, and M. M. Davis. 1991. Low affinity interaction of peptide-MHC complexes with T cell receptors. *Science 254:1788.*
48. Crawford, F., H. Kozono, J. White, P. Marrack, and J. Kappler. 1998. Detection of antigen-specific T cells with multivalent soluble class II MHC covalent peptide complexes. *Immunity 8:675.*
49. Savage, P. A., J. J. Boniface, and M. M. Davis. 1999. A kinetic basis for T cell receptor repertoire selection during an immune response. *Immunity 10:485.*
50. Fahmy, T. M., J. G. Bieler, M. Edidin, and J. P. Schneck. 2001. Increased TCR avidity after T cell activation: a mechanism for sensing low-density antigen. *Immunity 14:135.*
51. Rosette, C., G. Werlen, M. A. Daniels, P. O. Holman, S. M. Alam, P. J. Travers, N. R. Gascoigne, E. Palmer, and S. C. Jameson. 2001. The impact of duration versus extent of TCR occupancy on T cell activation: a revision of the kinetic proofreading model. *Immunity 15:59.*
52. Savage, P. A., and M. M. Davis. 2001. A kinetic window constricts the T cell receptor repertoire in the thymus. *Immunity 14:243.*
53. Busch, D. H., and E. G. Pamer. 1999. T cell affinity maturation by selective expansion during infection. *J. Exp. Med. 189:701.*
54. Constant, S., C. Pfeiffer, A. Woodard, T. Pasqualini, and K. Bottomly. 1995. Extent of T cell receptor ligation can determine the functional differentiation of naive CD4$^+$ T cells. *J. Exp. Med. 182:1591.*
55. Hemmer, B., I. Stefanova, M. Vergelli, R. N. Germain, and R. Martin. 1998. Relationships among TCR ligand potency, thresholds for effector function elicitation, and the quality of early signaling events in human T cells. *J. Immunol. 160:5807.*
56. Itoh, Y., and R. N. Germain. 1997. Single cell analysis reveals regulated hierarchical T cell antigen receptor signaling thresholds and intraclonal heterogeneity for individual cytokine responses of CD4$^+$ T cells. *J. Exp. Med. 186:757.*
57. Itoh, Y., B. Hemmer, R. Martin, and R. N. Germain. 1999. Serial TCR engagement and down-modulation by peptide:MHC molecule ligands: relationship to the quality of individual TCR signaling events. *J. Immunol. 162:2073.*
58. Tao, X., S. Constant, P. Jorritsma, and K. Bottomly. 1997. Strength of TCR signal determines the costimulatory requirements for Th1 and Th2 CD4$^+$ T cells differentiation. *J. Immunol. 159:5956.*
59. Carnaud, C., D. Lee, O. Donnars, S.-H. Park, A. Beavis, Y. Koezuka, and A. Bendelac. 1999. Cross-talk between cells of the innate immune system: NKT cells rapidly activate NK cells. *J. Immunol. 163:4647.*
60. Liu, H., M. Rhodes, D. L. Wiest, and D. A. Vignali. 2000. On the dynamics of TCR:CD3 complex cell surface expression and downmodulation. *Immunity 13:665.*
61. San Jose, E., A. Borroto, F. Niedergang, A. Alcover, and B. Alarcon. 2000. Triggering the TCR complex causes the downregulation of nonengaged receptors by a signal transduction-dependent mechanism. *Immunity 12:161.*
62. Valitutti, S., S. Muller, M. Salio, and A. Lanzavecchia. 1997. Degradation of T cell receptor (TCR)-CD3-ζ complexes after antigenic stimulation. *J. Exp. Med. 185:1859.*
63. Royer, W. E., Jr., J. E. Knapp, K. Strand, and H. A. Heaslet. 2001. Cooperative hemoglobins: conserved fold, diverse quaternary assemblies and allosteric mechanisms. *Trends Biochem. Sci. 26:297.*
64. Joyce, S., P. Tabaczewski, R. H. Angeletti, S. G. Nathenson, and I. Stroynowski. 1994. A non-polymorphic MHC class Ib molecule binds a large array of diverse self peptides. *J. Exp. Med. 179:579.*
65. Hartel, S., H. A. Diehl, and F. Ojeda. 1998. Methyl-β-cyclodextrins and liposomes as water-soluble carriers for cholesterol incorporation into membranes and its evaluation by a microenzymatic fluorescence assay and membrane fluidity-sensitive dyes. *Anal. Biochem. 258:277.*
66. Brown, D. A., and E. London. 2000. Structure and function of sphingolipid- and cholesterol-rich membrane rafts. *J. Biol. Chem. 275:17221.*
67. Fujii, S., K. Shimizu, M. Kronenberg, and R. M. Steinman. 2002. Prolonged IFN-γ-producing NKT response induced with α-galactosylceramide-loaded DCs. *Nat. Immunol. 3:867.*
68. Leitenberg, D., and K. Bottomly. 1999. Regulation of naive T cell differentiation by varying the potency of TCR signal transduction. *Semin. Immunol. 11:283.*
69. Baxter, A. G., S. J. Kinder, K. J. L. Hammond, R. Scollay, and D. I. Godfrey. 1997. Association between αβTCR$^+$CD4$^-$CD8$^-$ T-cell deficiency and IDDM in NOD/Lt mice. *Diabetes 46:572.*
70. Godfrey, D. I., S. J. Kinder, P. Silvera, and A. G. Baxter. 1997. Flow cytometric study of T cell development in NOD mice reveals a deficiency in αβTCR$^+$CDR$^-$CD8$^-$ thymocytes. *J. Autoimmun. 10:279.*
71. Hammond, K. J. L., L. D. Poulton, L. Palmisano, P. Silveira, D. I. Godfrey, and A. G. Baxter. 1998. α/β-T cell receptor (TCR)$^+$CD4$^-$CD8$^-$ (NKT) thymocytes prevent insulin-dependent diabetes mellitus in non-obese diabetic (NOD)/Lt mice by the influence of interleukin (IL)-4 and/or IL-10. *J. Exp. Med. 187:1047.*
72. Beaudoin, L., V. Laloux, J. Novak, B. Lucas, and A. Lehuen. 2002. NKT cells inhibit the onset of diabetes by impairing the development of pathogenic T cells specific for pancreatic β cells. *Immunity 17:725.*
73. Lehuen, A., O. Lantz, L. Beaudoin, V. Laloux, C. Carnaud, A. Bendelac, J. F. Bach, and R. C. Monteiro. 1998. Overexpression of natural killer T cells protects Vα14Jα281 transgenic nonobese diabetic mice against diabetes. *J. Exp. Med. 188:1831.*

74. Naumov, Y. N., K. S. Bahjat, R. Gausling, R. Abraham, M. A. Exley, Y. Koczuka, S. B. Balk, J. L. Strominger, M. Clare-Salzer, and S. B. Wilson. 2001. Activation of CD1d-restricted T cells protects NOD mice from developing diabetes by regulating dendritic cell subsets. *Proc. Natl. Acad. Sci. USA 98:13838.*
75. Chun, T., M. J. Page, L. Gapin, J. L. Matsuda, H. Xu, H. Nguyen, H. S. Kang, A. K. Stanic, S. Joyce, W. A. Koltun, et al. 2003. CD1d-expressing dendritic cells but not thymic epithelial cells can mediate negative selection of NKT Cells. *J. Exp. Med. 197:907.*
76. Call, M. E., J. Pyrdol, M. Wiedmann, and K. W. Wucherpfennig. 2002. The organizing principle in the formation of the T cell receptor-CD3 complex. *Cell 111:967.*
77. Wang, J., K. Lim, A. Smolyar, M. Teng, J. Liu, A. G. Tse, R. E. Hussey, Y. Chishti, C. T. Thomson, R. M. Sweet, et al. 1998. Atomic structure of an $\alpha\beta$ T cell receptor (TCR) heterodimer in complex with an anti-TCR Fab fragment derived from a mitogenic antibody. *EMBO J. 17:10.*
78. Ghendler, Y., A. Smolyar, H. C. Chang, and E. L. Reinherz. 1998. One of the CD3ϵ subunits within a T cell receptor complex lies in close proximity to the Cβ FG loop. *J. Exp. Med. 187:1529.*
79. Degermann, S., G. Sollami, and K. Karjalainen. 1999. T cell receptor β chain lacking the large solvent-exposed Cβ FG loop supports normal α/β T cell development and function in transgenic mice. *J. Exp. Med. 189:1679.*
80. Sasada, T., M. Touma, H. C. Chang, L. K. Clayton, J. H. Wang, and E. L. Reinherz. 2002. Involvement of the TCR Cβ FG loop in thymic selection and T cell function. *J. Exp. Med. 195:1419.*
81. Degermann, S., G. Sollami, and K. Karjalainen. 1999. Impaired NK1.1 T cell development in mice transgenic for a T cell receptor β chain lacking the large, solvent-exposed Cβ FG loop. *J. Exp. Med. 190:1357.*
82. Block, M. S., A. J. Johnson, Y. Mendez-Fernandez, and L. R. Pease. 2001. Monomeric class I molecules mediate TCR/CD3ϵ/CD8 interaction on the surface of T cells. *J. Immunol. 167:821.*

International Immunology, Vol. 16, No. 3, pp. 423–431
doi: 10.1093/intimm/dxh046

Development of TCRB CDR3 length repertoire of human T lymphocytes

Junko Nishio[1], Mihoko Suzuki[1], Toshihiro Nanki[1], Nobuyuki Miyasaka[1] and Hitoshi Kohsaka[1]

[1]Department of Bioregulatory Medicine and Rheumatology, Graduate School, Tokyo Medical and Dental University, 1-5-45 Yushima, Bunkyo-ku, Tokyo 113-8519, Japan

Keywords: gene rearrangement, peripheral blood, thymus

Abstract

The third complementarity-determining region (CDR3) of TCR interacts directly with antigenic peptides bound to grooves of MHC molecules. Thus, it is the most critical TCR structure in launching acquired immunity and in determining fates of developing thymocytes. Since length is one of the components defining the CDR3 heterogeneity, the CDR3 length repertoires have been studied in various T cell subsets from humans in physiological and pathological conditions. However, how the CDR3 length repertoire develops has been addressed only by a few reports, including one showing that CDR3 of CD4 thymocytes becomes shorter during thymic development. Here, we explored multiple regulations on the development of the TCRB CDR3 length repertoires in the thymus and the peripheral blood. CDR3 length spectratyping was employed to examine thymocyte and peripheral T cell populations for their CDR3 length repertoires. We have found that repertoire distribution patterns depend on use of the BV gene. The BV-dependent patterns were shaped during thymic selections and maintained in the peripheral blood. Differences in the mean CDR3 length among different BV subsets were seen throughout lymphocyte development. We also observed that CDR3 was shortened in both CD4 and CD8 thymocytes. Of note, the degrees of the shortening depended on the CD4/CD8 lineage and on use of the BV gene. When expansions of peripheral T cell clones are negligible, no obvious difference was seen between mature thymocytes and peripheral lymphocytes. Thus, the TCRB CDR3 length repertoires are finely tuned in the thymus before the lymphocytes emigrate into the peripheral blood.

Introduction

Using surface receptors for antigens, αβ T cells recognize antigenic peptides bound to MHC class I or II molecules. Studies using X-ray crystallography have demonstrated that three-dimensional structures composed by the first, second and third complementarity-determining regions (CDR1, 2 and 3) of TCR α and β chains interact directly with peptides presented by the MHC molecules (1,2). Avidity of the interaction is defined by topological structure and location of charged amino acid residues of the interface peptides (3). In the TCR chain, CDR3 nucleic acid sequence is most diverse because it is generated by recombination of multiple V, D (in the case of TCRβ) and J gene segments, and by random addition of interlocating N region nucleotides (4,5). Since this region interacts most closely with the antigenic peptide, the diversity of the CDR3 amino acid sequences accounts for a wide array of antigen specificities within the functional T cell repertoire.

The molecular interaction of interface peptides is similarly important in association between antigenic peptides and MHC molecules. This interaction limits heterogeneity of peptides that can bind to the products of a given MHC allele (6). The length of the antigenic peptides is also restricted by interaction with MHC and with TCR (6). In contrast, the TCR CDR3 segments are more diverse in length. This might be explained by weaker association of antigenic peptides with TCR than with MHC (3,7). However, it remains to be seen how the CDR3 length repertoire is regulated during thymic development and in peripheral blood.

The αβ T cell repertoire develops through a number of selection steps in the thymus. TCRB gene rearrangement becomes complete first at the stage of $CD3^-CD4^+CD8^-$ immature single-positive (CD4 ISP) thymocytes (8,9). If their TCRB genes rearrange in-frame and their products pair successfully with pre-Tα chains, these cells survive and

Correspondence to: H. Kohsaka; E-mail: kohsaka.rheu@tmd.ac.jp

Transmitting editor: K. Yamamoto

Received 25 August 2003, *accepted* 25 November 2003

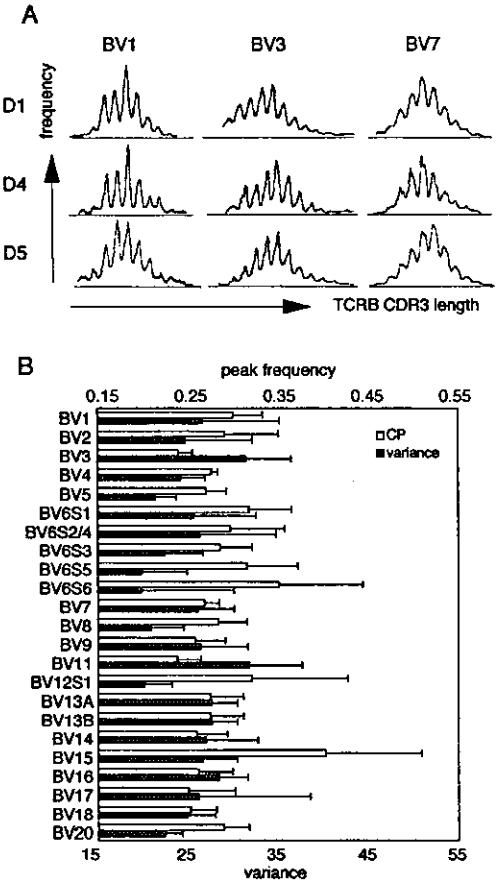

Fig. 1. BV-dependent differences in TCRB CLS histogram. (A) The histograms of the BV1, 3 and 7 subsets of peripheral CD4 T cells from three donors (D1, D4 and D5). (B) The CP frequencies and the variances in the individual BV subsets. They were calculated using TCRB CLS histograms of peripheral CD4 T cells from six child donors. The classification of the BV families was based on the definition by the WHO/International Union of Immunological Societies, Nomenclature Subcommittee on TCR Designation (30). The open columns and shaded columns represent the mean values of the CP frequencies and those of the variances respectively. The bars show their SD.

proliferate to become CD4⁺CD8⁺ double-positive thymocytes (8,10). They express TCRβ chains together with products of the in-frame rearranged TCRA gene. The double-positive thymocytes then undergo positive and negative selection, which make mature CD4 and CD8 T cell repertoires desirable to eliminate foreign pathogens. Although these processes are directed by the avidity of TCR with its ligand (11), their effects on the CDR3 length repertoire have hardly been explored.

The heterogeneity of the TCR CDR3 length in T cells at any developmental stages can be tested with TCR CDR3 length spectratyping (CLS). This method visualizes the distribution of TCR CDR3 length as histograms (12). It has been shown that typical histograms that are derived from mature peripheral T lymphocyte pools display a Gaussian-like distribution with 3-base spacing. If a histogram is biased by an unexpectedly high frequency at a specific length, it indicates that the studied population contains an expanded T cell clone whose CDR3 has the corresponding length. Based on this, the TCR CLS technique has been employed to study clonal perturbation of T cell repertoires from healthy donors and patients with various inflammatory diseases (13–19). The results have given us some insights into the physiology and pathology of T cell homeostasis.

The above facts all indicate the importance of discerning how heterogeneity of the CDR3 length repertoire is physiologically regulated, especially in the thymus. No gross difference in CDR3 length distribution between fetal and adult T cell pools has been reported (20). Yassai *et al.* (21) reported that thymocytes with shorter TCRB CDR3 are selected during transition from CD4⁺CD8⁺ thymocytes to CD4 SP thymocytes. Their subsequent report used murine systems to show that the shortening is mediated by TCR–peptide–MHC interaction in the thymus (22). Of note, they suggested that human repertoires might be under distinct regulation. Other investigators have described that different TCRB CDR3 lengths were preferred by different BV and BJ combinations in mice (23), and BJ genes in humans (24). However, no studies have addressed which stages in lymphocyte development are responsible for these differences.

How are the CDR3 length repertoires of various T cell subsets formed, modulated and maintained in the thymus and in the peripheral blood? How does the shortening occur in the human thymus? The present study was conducted to address these issues. By examining thymocytes and peripheral T cells for TCR CLS patterns, we have found that formation of human TCR CDR3 length repertoires is under multiplex regulations in the thymus.

Methods

Samples

Thymic fragments and peripheral blood were collected from child donors during heart surgery for correction of congenital cardiac anomalies. They were from 1 to 13 years old (mean 5.6 years old). They suffered from no immunological or hematological disorders. Consent forms were obtained before the operation. CD4 ISP thymocytes, mature CD4 and CD8 SP thymocytes, and peripheral CD4 and CD8 T lymphocytes were sorted from the thymic tissues or peripheral lymphocytes as described previously (25). Purities of the separated cells were >94%.

PCR

RNA were extracted from the sorted thymocytes and lymphocytes, and converted to cDNA (25). To amplify TCR transcripts with individual TCRBV family genes, the cDNA were subjected to PCR using a fluorescent TCRBC-specific anti-sense primer (C_βb) and a panel of sense oligonucleotide primers specific to TCRBV gene families (26). The amplification reaction consisted of 35 cycles of 1 min at 94°C, 1 min at 60°C and 1 min at 72°C, with final extension at 72°C for 7 min.

To amplify TCR transcripts with individual members of the BV7 family (BV7S1, BV7S2 and BV7S3 genes), a sense primer specific to the three BV7 family genes (V_β7os: GGA GCT CAT

GTT TGT CTA CA) and a BC-specific antisense primer [C_βa (26)] were used for primary PCR. The reaction consisted of 25 cycles of 1 min at 94°C, 1 min at 53°C and 1 min at 72°C followed by final extension at 72°C for 7 min. Part of the products were further amplified with a nested sense primer specific to BV7S1, BV7S2 or BV7S3 genes (V_β7S1s: TAC AGC TAT GAG AAA CTC TC; V_β7S2s: TAC AGT CTT GAA GAA CGG GT; or V_β7S3s: TCT ACA ACT TTA AAG AAC AGA C) and the fluorescent C_βb primer. The reaction consisted of 25 cycles of 1 min at 94°C, 1 min at 53°C and 1 min at 72°C followed by final extension at 72°C for 7 min.

TCR CLS

The PCR products were fractionated on denaturing 7% polyacrylamide gel in a Hitachi SQ-5500 sequencer (Hitachi Electronics Engineering, Tokyo, Japan). The data were analyzed with the associated software to display histograms. Relative percentage of the TCRB transcripts of a given length to total TCRB transcripts in the BV subsets, which is called the frequency in this report, was calculated by dividing the fluorescence intensity of the corresponding peaks by the sum of the intensity of all peaks.

Statistical analyses

CDR3 length, defined as previously described (20), ranged from 6 to 60 bases. Nineteen frequency values within this range were treated as variables for cluster analyses, which were performed with Statistica 4.1J (Tulsa, OK). The variances were calculated as follows: $\sum_{n=2}^{20} F_{3n} \times (L_{3n} - \text{mean CDR3 length})^2$, where F_{3n} stands for the frequency value that corresponds to a given CDR3 length of L_{3n}. The Kruskal–Wallis test was used to compare the central peak (CP) frequencies, variances and mean CDR3 lengths of the histograms of different BV subsets. The Mann–Whitney test was used to compare these parameters of the histograms of the CD4 ISP thymocytes with those of the other populations.

Results

BV-dependent TCRB CDR3 length repertoires of peripheral CD4 T cells

In order to characterize unbiased TCRB CDR3 length repertoires of the mature T lymphocytes, peripheral CD4 T lymphocytes from six child donors were examined. This population was studied because biases of the T cell repertoires by clonally expanded T cells are more frequent in elder individuals and in the CD8 T cell pool (13,15,27,28). Although the histogram of each BV subset displayed a Gaussian-like distribution without outstanding biases, different BV subsets had slightly different patterns. Histograms of BV1, 3 and 7 gene families of three donors are shown to represent such differences (Fig. 1A). The shapes of different BV subsets were distinguished by the height of the CP that always had the highest frequency and by the width of the span. The histograms of BV1 had a high CP and narrow span, those of BV3 had a low CP and wide span, and BV7 had modestly high CP and a narrow span.

The characteristics were quantitatively assessed with the CP frequencies and the variances; the variances indicate span of the histograms. These two values were calculated for all BV subsets studied (Fig. 1B). Various combinations of CP frequencies and variances were observed. Reflecting the histogram pattern of the BV3 subset, its CP frequencies were low and the variances were remarkably large. This was also the case with the BV11 subset. The BV1 subset, as well as the BV6S1 subset, had high CP frequencies and small variances. The two parameters also describe the characteristics of the BV7 subset: moderate CP frequency and small variance.

Although some BV subsets had higher CP frequencies than BV1, or smaller variances than BV1 and 7, the BV1, 3 and 7 subsets were further studied to investigate how these differences develop during T lymphocyte development. The other BV subsets occasionally had minor and random biases, which should be due to small expansions of T cell clones. The characteristics of the three BV subsets and similarity within the same subsets could be illuminated by line graphs of the CDR3 length repertoires from six donors (Fig. 2A). Statistical comparison of the CP frequencies and the variances among the three subsets from six donors demonstrated that the CP frequencies of the BV1 subset were highest, while those of the BV3 subset were lowest, and that the variances in the BV3 subset were largest (Fig. 3A and B).

Pannetier *et al.* (23) reported that the mean TCRB CDR3 length of murine lymphocytes depends on use of BV genes. This was the case with human peripheral lymphocytes; the mean length of the TCRBV7 transcripts was longest, while that of the TCRBV3 transcripts was shortest (Fig. 3C).

Overall differences in the CLS patterns were elucidated by cluster analysis, which treated 19 frequency values at 6–60 bases as variables. A total of 18 histograms from six donors were segregated into three groups, each of which contained histograms of BV1, 3 or 7 subsets (Fig. 4A).

According to the published database, the BV7 family consists of BV7S1, 7S2 and 7S3 genes, while BV1 and 3 families have a single gene member (29). The histograms of the BV7 subset were derived from the PCR products that were generated with a primer specific to all BV7 family genes. In order to examine the TCR transcripts with individual BV7 genes, these transcripts were independently amplified with specific primers. The CLS distributions of the transcripts with the three BV7 genes were homologous and no statistical differences in CP frequency, variance or mean TCR length were observed (data not shown). Thus, the BV7 family subset was analyzed as a whole in the present studies.

Development of the BV-dependent repertoires in the thymus

TCRBV1, 3 and 7 transcripts that were derived from CD4 ISP thymocytes, and CD4 and CD8 SP thymocytes from the same set of donors were analyzed to study how the BV-dependent characteristics develop. As was discussed in our previous report (25), the CD4 ISP thymocytes have undergone TCRB gene rearrangement, but have not started positive or negative selection. Thus, unlike CD4 CD8 double-positive cells, a part of which are already under pressure of thymic selection, they are the best for investigation of primordial TCR repertoires.

The histograms of the CD4 and CD8 SP thymocytes shared the same characteristics as those of the peripheral CD4 cells

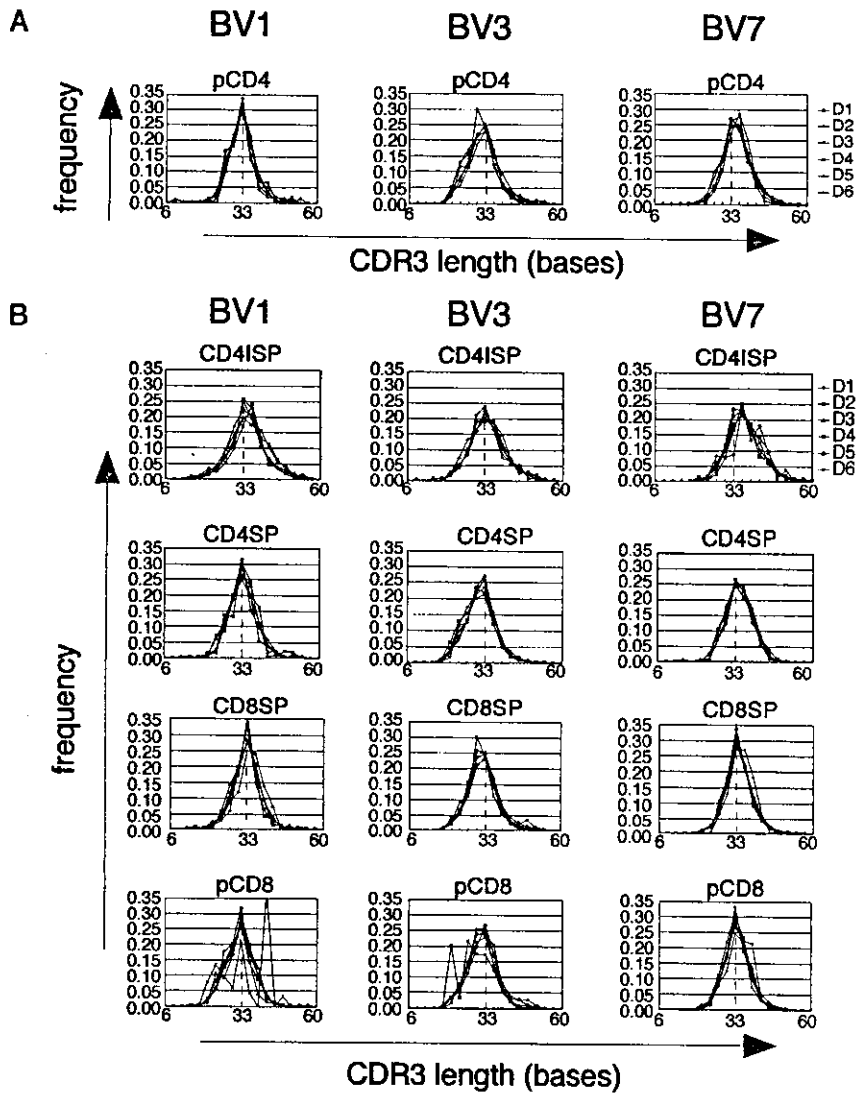

Fig. 2. TCRB CLS histograms of the BV1, 3 and 7 subsets of the peripheral lymphocytes and thymocytes. Distributions of the frequencies are presented in a line graph format. The data of the six donors (D1–D6) are shown as overlaid line graphs in each panel to illuminate BV-specific characteristics. (A) The histograms of the three BV subsets in their peripheral CD4 T cells. (B) The histograms of the CD4 ISP, CD4 SP and CD8 SP thymocytes, and peripheral CD8 T cells. Except for the CD4 ISP thymocytes, the histograms of each BV subset were similar. The BV1 and 3 subsets of the peripheral CD8 T cells from D4 were considerably biased, probably because of clonal expansions.

(Fig. 2B). In both SP populations, the CP frequencies of the BV1 subset were highest and those of the BV3 subset were lowest. The variances in the BV3 subset were largest. These differences were statistically significant (Fig. 3A and B).

Peripheral CD8 T cells from the same donors were analyzed in the same way. Their histograms were often biased since CD8 T cells are prone to large clonal expansions. Nevertheless, the BV-dependent characteristics were held well by the peripheral CD8 T cells (Figs 2B, and 3A and B).

In contrast, differences among the three subsets were not significant in the histograms of the CD4 ISP thymocytes (Fig. 2B). These histograms shared the same features, which were characterized by low CP and wide span regardless of BV gene use. In all of the three BV subsets, the CP frequencies and variances of the CD4 ISP thymocytes were different from those of the SP thymocytes and peripheral T cells in a statistically significant manner (Fig. 3A and B). The CP frequencies of CD4 ISP were significantly lower than those of CD4 SP in the BV1, 3, and 7 subsets ($P < 0.01$, $P < 0.05$ and $P < 0.05$ respectively), than those of CD8 SP ($P < 0.01$ for each subset), than those of peripheral CD4 ($P < 0.01$, $P < 0.05$ and $P < 0.01$ respectively) and than those of peripheral CD8 ($P < 0.01$, $P < 0.05$ and $P < 0.01$ respectively). The variances of CD4 ISP were significantly larger than those of CD4 SP in the

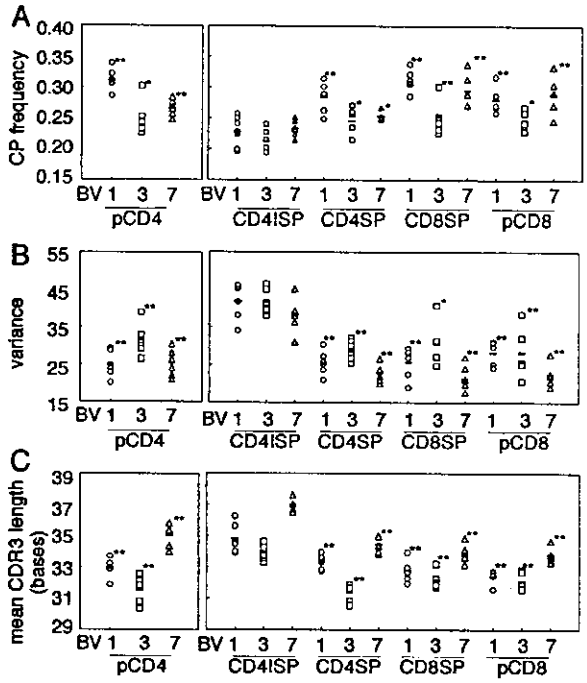

Fig. 3. Parameters to compare the TCR CLS histograms of CD4 ISP, CD4 SP and CD8 SP thymocytes, and peripheral CD4 and CD8 T cells. CP frequencies (A), variances (B) and mean CDR3 lengths (C) in the BV1, 3 and 7 subsets from the six donors are shown. Those of the peripheral CD8 T cells from D4 are excluded because of obvious biases. The Kruskal–Wallis test was used to compare the three parameters among the BV subsets. In the peripheral CD4, the three subsets were statistically different with respect to the CP frequency ($P < 0.005$), the variance ($P < 0.05$) and the mean CDR3 length ($P < 0.001$). In the CD4 ISP thymocytes, the three BV subsets were not significantly different with respect to the CP frequency and the variance, but significantly different with respect to the CDR3 length ($P < 0.002$). In the CD4 SP and CD8 SP thymocytes, the three BV subsets were different with respect to the CP frequency ($P < 0.05$ for both), the variances ($P < 0.02$ for both) and the mean CDR3 length ($P < 0.001$ and $P < 0.005$ respectively). The three BV subsets from peripheral CD8 were different with respect to the CP frequency ($P < 0.05$), the variance ($P < 0.05$) and the mean CDR3 length ($P < 0.005$). The Mann–Whitney test was used to compare the three parameters of the CD4 ISP thymocytes and the other populations. The CP frequencies of CD4 ISP were always lower than those of CD4 SP in the BV1, 3 and 7 subsets, than those of CD8 SP, than those of peripheral CD4, and than those of peripheral CD8. The variances of CD4 ISP were larger than those of CD4 SP in the BV1 3 and 7 subsets, than those of CD8 SP, than those of peripheral CD4, and than those of peripheral CD8. The mean CDR3 lengths of CD4 ISP were longer than those of CD4 SP, CD8 SP, peripheral CD4, and peripheral CD8 in all three subsets. $^{*}P < 0.05$ and $^{**}P < 0.01$ respectively in the Mann–Whitney test to compare each T cell population with the corresponding CD4 ISP population.

BV1, 3 and 7 subsets ($P < 0.01$ for each subset), than those of CD8 SP ($P < 0.01$, $P < 0.05$, and $P < 0.01$ respectively), than those of peripheral CD4 ($P < 0.01$ for each subset) and than those of peripheral CD8 ($P < 0.01$ for each subset).

As for the mean CDR3 length, the same differences among the three BV subsets were observed in the CD4 and CD8 SP thymocytes, and in the peripheral CD8 T cells (Fig. 3C). Unlike the distribution patterns, the differences in length were already seen in the CD4 ISP thymocytes (Fig. 3C). These results imply that positive and negative selections exert distinct effects on CLS distribution pattern and on CDR3 length.

Cluster analyses segregated the histograms of the CD4 and CD8 SP thymocytes into three groups, each of which contained primarily those of the same BV subset (Fig. 4C and D). The histograms of the peripheral CD8 T cells also fell into the three groups except for the histograms with biases (Fig. 4B). Notably, the same analysis of the histograms of the ISP thymocytes failed to discriminate BV gene use (Fig. 4E). This should be due to similarity of the distribution patterns and suggests that the difference in length alone is not enough for segregation.

BV- and co-receptor-dependent shortening of TCRB CDR3 length in the human thymus

It has been reported that TCR CDR3 shortens during transition from the ISP thymocytes to the SP thymocytes (21). This was observed in our studies of the mean CDR3 length; the CD4 ISP thymocytes had longer CDR3 than the other populations (Fig. 3C). To investigate this further, we analyzed plots of differences in frequency (ΔF) and skew values ($\Sigma\Delta F$), both of which have been defined by Yassai *et al.* (21,22). ΔF can be calculated by subtracting the CLS frequency of a given population from that of the other at the same length. A cluster of positive ΔF values on the right of an inflection point with a corresponding cluster of negative ΔF values on the other side indicates that the given population has shorter CDR3. $\Sigma\Delta F$ is the sum of ΔF values to the right of the inflection points. The ΔF plots and $\Sigma\Delta F$ were calculated by subtraction of the frequencies of the CD4 and CD8 SP thymocytes from those of the CD4 ISP thymocytes in the three BV subsets (Fig. 5A). Their patterns and positive $\Sigma\Delta F$ values showed that both SP thymocyte populations had shorter CDR3 than the CD4 ISP thymocytes irrespective of BV subset.

Interaction of TCR with endogenous antigens dictates CD4/CD8 lineage commitment during positive and negative selections in the thymus. This led us to assume that the shortening could be a function of the lineage if it is a consequence of TCR triggering. We then calculated ΔF between cells with different lineages; between the CD4 and CD8 SP thymocytes and between the peripheral CD4 and CD8 T cells (Fig. 5B). The ΔF plots and $\Sigma\Delta F$ showed that the TCR CDR3 length of CD4 lineage cells was shorter in the BV3 subset, whereas it was longer in the BV7 subset. No significant differences in CDR3 length were seen in the BV1 subset. Thus, differential shortening between CD4 and CD8 lineage cells was observed and it depended on BV gene use.

Additionally, the CD4 SP thymocytes and the peripheral CD4 T lymphocytes, as well as the CD8 SP thymocytes and the peripheral CD8 T lymphocytes, were compared. The results showed that CDR3 of CD4 or CD8 lineage cells do not shorten in the peripheral blood (data not shown).

Discussion

The present study has elucidated how TCR CDR3 length repertoires of CD4 and CD8 T cells in different BV subsets develop in the human thymus and peripheral blood. The CDR3 length repertoires had BV-dependent distribution patterns.

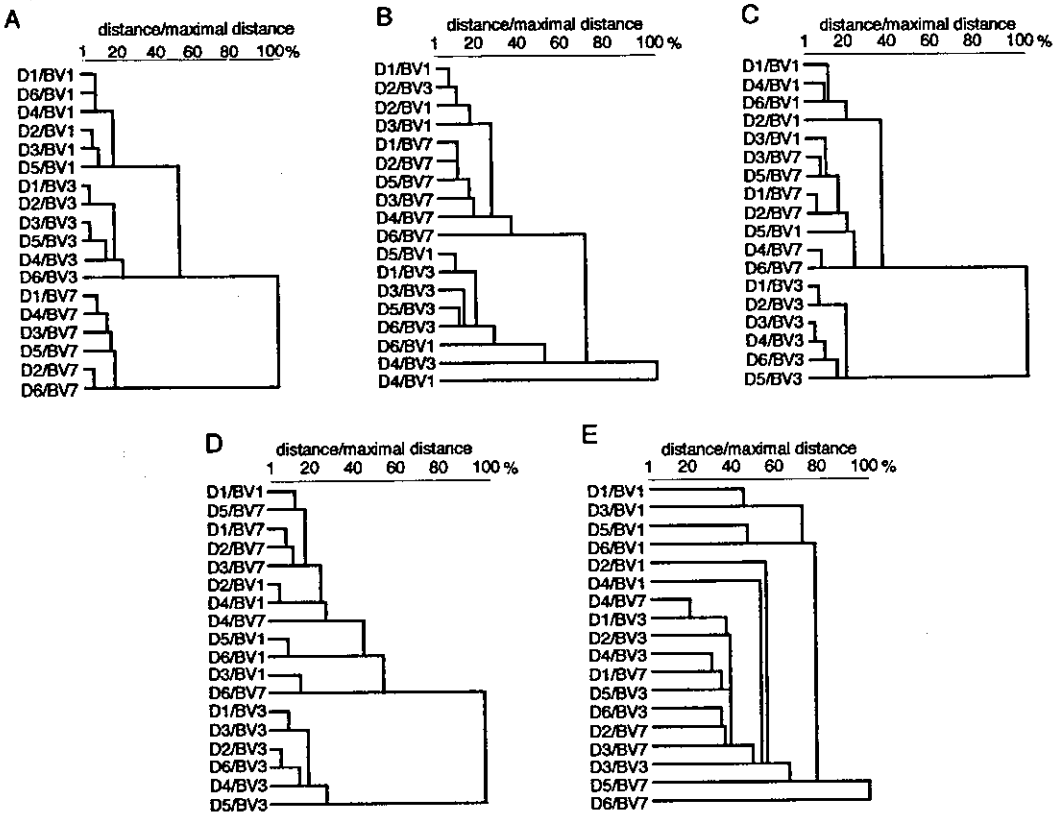

Fig. 4. Cluster analyses of the histograms of individual T cell populations from the six donors. Based on 18 histograms of peripheral CD4 (A) and CD8 (B) T cells, CD4 SP (C) and CD8 SP (D) thymocytes, and CD4 ISP thymocytes (E), the distance of every combination of two histograms was calculated with Ward's method and the Euclidean distance. All calculated distances divided by the maximal distance are shown in a dendrogram. Listed on the left are the BV subsets and the identification of donors that the individual histograms originated from. The BV1 and 3 subsets of the peripheral CD8 T cells from D4 had biased CLS histograms.

They were shaped during thymic selections and maintained in the peripheral blood. In contrast, the BV-dependent differences in the TCR CDR3 length were observed throughout lymphocyte development. The CDR3 became shorter during thymic selections, but did not change the BV-dependent differences seen before the selections. Finally, the degrees of the shortening differed between CD4 and CD8 lineage cells, and also were dependent on BV gene use. The repertoires of peripheral lymphocytes reflected directly those of mature SP thymocytes except for biases induced by clonal expansions.

Although it was known that different CDR3 lengths were preferred by different BV subsets, the BV-dependent distribution patterns are disclosed here for the first time. Unlike the difference in length, the different patterns become evident during positive and negative selections, accompanied by an increase of the CP frequency and narrowing of the distribution span. This argues that they are shaped under the pressure of positive and negative selections in the thymus. Most studies that employed the TCR CLS technique disregarded the differences, probably because the technique was used for identification of gross changes.

We have found that the distribution patterns of three gene members of the BV7 family shared the same characteristics. This ensures that the CLS histograms generated with the primer specific to BV7 family genes were not artifacts. In this regard, we have found that different gene members of the BV6 family could have similar distribution patterns (Fig. 1B). Also, both BV3 and 11 subsets shared histograms with low CP frequencies and large variances. Arden *et al.* (29) pointed out that these two genes are closely related both structurally and in their CDR3 sequences. According to their TCRBV gene classification, BV1, 3 and 7 fall into different groups. These facts argue that the BV-dependent differences could be attributable to the structure of TCRβ chains.

Using murine thymus, Pannetier *et al.* (23) observed that different BV subsets prefer different TCR CDR3 lengths. We found that the BV-dependent difference in mean TCR length already occurred in the CD4 ISP thymocytes. This implies that the difference is regulated by TCR rearrangement. Also, since the CD4 ISP thymocytes with complete TCRB gene rearrangement are under pressure of subsequent β selection for association with pre-Tα chains, the β selection could contribute to the difference formation. Moreover, the CLS histograms

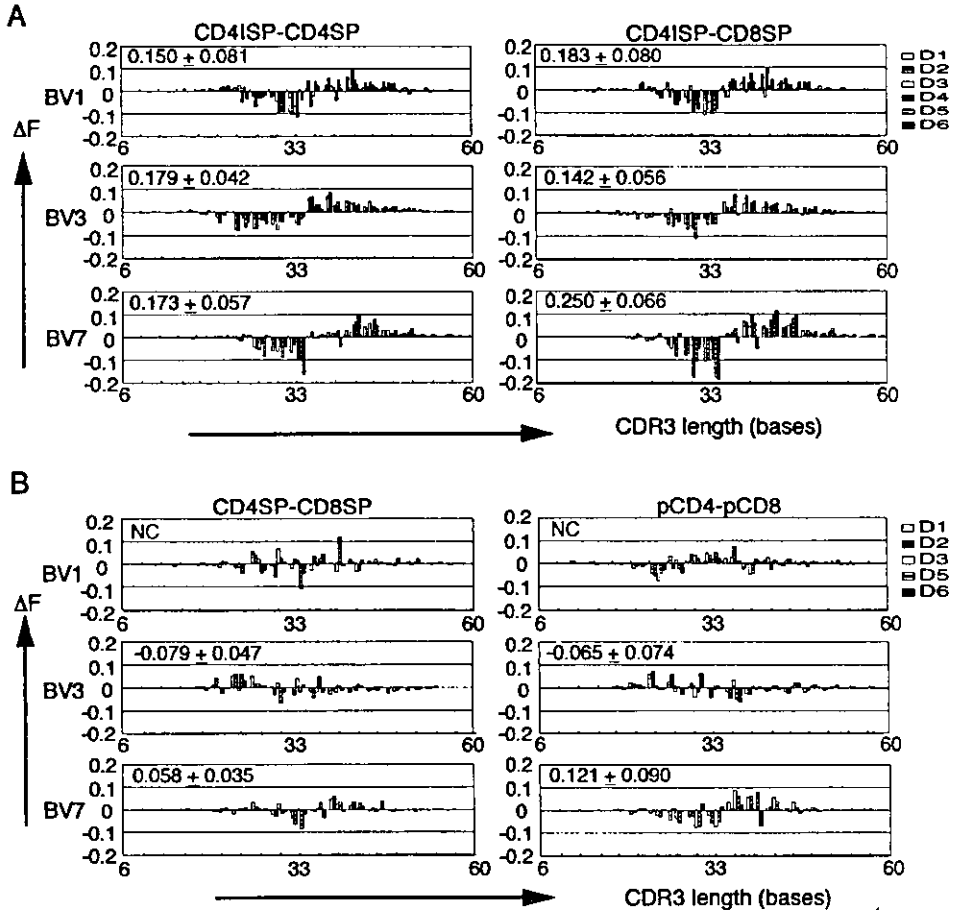

Fig. 5. Comparison of TCR CDR3 length in different CD4/CD8 lineage cells. Plotted are ΔF that were calculated by subtracting the frequencies in the CD4 and CD8 SP thymocytes from those in the ISP thymocytes (A: CD4 ISP – CD4 SP and CD4 ISP – CD8 SP respectively), and by subtracting the frequencies in the CD8 SP thymocytes from those in the CD4 SP thymocytes and those in the peripheral CD8 T cells from those in the peripheral CD4 T cells (B: CD4 SP – CD8 SP and peripheral CD4 – peripheral CD8 respectively). In order to quantify the shortening, the means ± SD of $\Sigma\Delta F$ derived from the six donors were calculated (shown in the panels). In (B), where the data from D4 have been excluded, $\Sigma\Delta F$ values of the BV3 subsets were all negative in both subtractions, while $\Sigma\Delta F$ values of the BV7 subsets were all positive. $\Sigma\Delta F$ values were not calculated for the BV1 subset because no inflection points were found in the ΔF plots. NC, not calculated.

of the BV1, 3 and 7 subsets of the CD4 ISP thymocytes were similar, but not necessarily identical (Fig. 2B), suggesting that the rearrangement and/or β selection may have a subsidiary effect in shaping the CLS distribution patterns.

To address further if the rearrangement *per se* regulates the BV-dependent difference in CDR3 length, we tried to amplify non-productively recombined TCRBV1, 3 and 7 genes from peripheral T lymphocytes that do not express TCRVβ1, 3 or 7. However, even from $>10^7$, a sufficient amount of the rearranged genes could not be amplified for the TCR CLS analyses. This was consistent with the fact that the TCRB CLS patterns of the CD4 ISP thymocytes always had 3-base pair spacing, indicating that all transcripts were in-frame. The 3-base spacing was also observed by Yassai *et al.* (21) who examined TCRB genomic DNA derived from the same population. It is known that 85% of CD4 ISP thymocytes retain the TCRB germline configuration, while only 5% express rearranged TCRB gene products (9). Thus, thymocytes with out-of-frame TCRB rearrangements must be diluted out quickly by those expressing complete TCRβ/pre-Tα and become undetectable with conventional technologies.

In separate experiments, we have assessed the mean TCR CDR3 lengths of the other BV subsets and found that the BV subsets with similar CLS patterns do not necessarily have similar CDR3 length (data not shown). The differences in shortening between CD4 and CD8 lineage cells were not a function of the distribution patterns (data not shown). Thus, distribution pattern and length appeared to be regulated independently.

Yassai *et al.* (21,22) reported TCR shortening in the human and murine thymi. By examining murine thymocytes for the BV1–BJ2 recombinants, they have shown that the shortening

occurs to a larger extent in the CD4 lineage cells than in the CD8 lineage cells. They failed to see differential shortening in humans and suggested a distinct regulation for human thymocytes. However, we observed a clear difference between the CD4 and CD8 T cells. We found that the differential shortening was a function of BV gene use. These data imply that the shortening in humans is regulated by antigen recognition by TCR.

The TCR shortening could be affected by allelic variations of MHC gene products, and differential shortening between CD4 and CD8 lineage cells could be due to differential orthogonal geometry of TCR and antigenic peptide in the grooves of MHC class I and II molecules (22). However, the differences in mean CDR3 length were preserved throughout the thymic selections. The CD4 and CD8 lineage cells share the same CLS distribution patterns. Thus, although limitations in sample collection did not allow us to investigate the effects of HLA variations, the geometry should not be the only factor regulating CDR3 length repertoire.

Development of the TCRB CDR3 length repertoire is regulated delicately in the thymus. Peripheral selections have little effect unless T cell clones expand massively in response to immunological insults. Elucidation of these thymic regulations may shed more light on molecular interaction of TCR with self-peptide–MHC in the thymus.

Acknowledgements

This study was supported by a grant from the Ministry of Health, Labor and Welfare, Japan. The authors thank Dr Takeshi Hiramatsu at Tokyo Women's Medical University for providing us with thymus and peripheral blood samples.

Abbreviations

ΔF	differences in frequency
$\Sigma\Delta F$	skew value
CDR	complementarity-determining region
CLS	CDR3 length spectratyping
CP	central peak
ISP	immature single positive
SP	single positive

References

1 Garboczi, D. N., Ghosh, P., Utz, U., Fan, Q. R., Biddison, W. E. and Wiley, D. C. 1996. Structure of the complex between human T-cell receptor, viral peptide and HLA-A2. *Nature* 384:134.
2 Garcia, K. C., Degano, M., Stanfield, R. L., Brunmark, A., Jackson, M. R., Peterson, P. A., Teyton, L. and Wilson, I. A. 1996. An αβ T cell receptor structure at 2.5 Å and its orientation in the TCR–MHC complex. *Science* 274:209.
3 Jorgensen, J. L., Reay, P. A., Ehrich, E. W. and Davis, M. M. 1992. Molecular components of T-cell recognition. *Annu. Rev. Immunol.* 10:835.
4 Wilson, R. K., Lai, E., Concannon, P., Barth, R. K. and Hood, L. E. 1988. Structure, organization and polymorphism of murine and human T-cell receptor α and β chain gene families. *Immunol. Rev.* 101:149.
5 Davis, M. M. 1990. T cell receptor gene diversity and selection. *Annu. Rev. Biochem.* 59:475.
6 Rammensee, H. G. 1995. Chemistry of peptides associated with MHC class I and class II molecules. *Curr. Opin. Immunol.* 7:85.
7 Matsushita, S., Takahashi, K., Motoki, M., Komoriya, K., Ikagawa, S. and Nishimura, Y. 1994. Allele specificity of structural requirement for peptides bound to HLA-DRB1*0405 and -DRB1*0406 complexes: implication for the HLA-associated susceptibility to methimazole-induced insulin autoimmune syndrome. *J. Exp. Med.* 180:873.
8 Ramiro, A. R., Trigueros, C., Marquez, C., San Millan, J. L. and Toribio, M. L. 1996. Regulation of pre-T cell receptor (pTα-TCRβ) gene expression during human thymic development. *J. Exp. Med.* 184:519.
9 Blom, B., Verschuren, M. C., Heemskerk, M. H., Bakker, A. Q., van Gastel-Mol, E. J., Wolvers-Tettero, I. L. M., van Dongen, J. J. M. and Spits, H. 1999. TCR gene rearrangements and expression of the pre-T cell receptor complex during human T-cell differentiation. *Blood* 93:3033.
10 Fehling, H. J., Krotkova, A., Saint-Ruf, C. and von Boehmer, H. 1995. Crucial role of the pre-T-cell receptor α gene in development of αβ but not γδ T cells. *Nature* 375:795.
11 Sebzda, E., Mariathasan, S., Ohteki, T., Jones, R., Bachmann, M. F. and Ohashi, P. S. 1999. Selection of the T cell repertoire. *Annu. Rev. Immunol.* 17:829.
12 Pannetier, C., Even, J. and Kourilsky, P. 1995. T-cell repertoire diversity and clonal expansions in normal and clinical samples. *Immunol. Today* 16:176.
13 Hingorani, R., Choi, I. H., Akolkar, P., Gulwani, A. B., Pergolizzi, R., Silver, J. and Gregersen, P. K. 1993. Clonal predominance of T cell receptors within the CD8+ CD45RO+ subset in normal human subjects. *J. Immunol.* 151:5762.
14 Gorski, J., Yassai, M., Zhu, X., Kissela, B., Keever, C. and Flomenberg, N. 1994. Circulating T cell repertoire complexity in normal individuals and bone marrow recipients analyzed by CDR3 size spectratyping. Correlation with immune status. *J. Immunol.* 152:5109.
15 Schwab, R., Szabo, P., Manavalan, J. S., Weksler, M. E., Posnett, D. N., Pannetier, C., Kourilsky, P. and Even, J. 1997. Expanded CD4+ and CD8+ T cell clones in elderly humans. *J. Immunol.* 158:4493.
16 Maccalli, C., Farina, C., Sensi, M., Parmiani, G. and Anichini, A. 1997. TCR β-chain variable region-driven selection and massive expansion of HLA-class I-restricted antitumor CTL lines from HLA-A*0201+ melanoma patients. *J. Immunol.* 158:5902.
17 Lin, M. Y. and Welsh, R. M. 1998. Stability and diversity of T cell receptor repertoire usage during lymphocytic choriomeningitis virus infection of mice. *J. Exp. Med.* 188:1993.
18 Sourdive, D. J., Murali, K. K., Altman, J. D., Zajac, A. J., Whitmire, J. K., Pannetier, C., Kourilsky, P., Evavold, B., Sette, A. and Ahmed, R. 1998. Conserved T cell receptor repertoire in primary and memory CD8 T cell responses to an acute viral infection. *J. Exp. Med.* 188:71.
19 Nishio, J., Suzuki, M., Miyasaka, N. and Kohsaka, H. 2001. Clonal biases of peripheral CD8 T cell repertoire directly reflect local inflammation in polymyositis. *J. Immunol.* 167:4051.
20 Moss, P. A. and Bell, J. I. 1995. Sequence analysis of the human αβ T-cell receptor CDR3 region. *Immunogenetics* 42:10.
21 Yassai, M. and Gorski, J. 2000. Thymocyte maturation: selection for in-frame TCR α-chain rearrangement is followed by selection for shorter TCR β-chain complementarity-determining region 3. *J. Immunol.* 165:3706.
22 Yassai, M., Ammon, K., Goverman, J., Marrack, P., Naumov, Y. and Gorski, J. 2002. A molecular marker for thymocyte-positive selection: selection of CD4 single-positive thymocytes with shorter TCRB CDR3 during T cell development. *J. Immunol.* 168:3801.
23 Pannetier, C., Cochet, M., Darche, S., Casrouge, A., Zoller, M. and Kourilsky, P. 1993. The sizes of the CDR3 hypervariable regions of the murine T-cell receptor β chains vary as a function of the recombined germ-line segments. *Proc. Natl Acad. Sci. USA* 90:4319.
24 Hall, M. A. and Lanchbury, J. S. 1995. Healthy human T-cell receptor β-chain repertoire. Quantitative analysis and evidence for J β-related effects on CDR3 structure and diversity. *Hum. Immunol.* 43:207.
25 Nanki, T., Kohsaka, H. and Miyasaka, N. 1998. Development of human peripheral TCRBJ gene repertoire. *J. Immunol.* 161:228.
26 Kohsaka, H., Taniguchi, A., Chen, P. P., Ollier, W. E. R. and

Carson, D. A. 1993. The expressed T cell receptor V gene repertoire of rheumatoid arthritis monozygotic twins:rapid analysis by anchored polymerase chain reaction and enzyme-linked immunosorbent assay. *Eur. J. Immunol.* 23:1895.

27 Callahan, J. E., Kappler, J. W. and Marrack, P. 1993. Unexpected expansions of CD8-bearing cells in old mice. *J. Immunol.* 151:6657.

28 Novak, E. J., Liu, A. W., Nepom, G. T. and Kwok, W. W. 1999. MHC class II tetramers identify peptide-specific human CD4+ T cells proliferating in response to influenza A antigen. *J. Clin. Invest.* 104:R63.

29 Arden, B., Clark, S. P., Kabelitz, D. and Mak, T. W. 1995. Human T-cell receptor variable gene segment families. *Immunogenetics* 42:455.

30 Williams, A. F., Strominger, J. L., Bell, J., Mak, T. W., Kappler, J., Marrack, P., Arden, B., Lefranc, M. P., Hood, L., Tonegawa, S. and Davis, M. 1993. Nomenclature for T-cell receptor (TCR) gene segments of the immune system. *WHO Bull.* 71:113.

Gene Transfer of a Cell Cycle Modulator Exerts Anti-Inflammatory Effects in the Treatment of Arthritis[1]

Yoshinori Nonomura, Hitoshi Kohsaka,[2] Kenji Nagasaka, and Nobuyuki Miyasaka

Forced expression of a cyclin-dependent kinase inhibitor gene, $p21^{Cip1}$ in the synovial tissues was effective in treating animal models of rheumatoid arthritis. Synovial hyperplasia in the treated joints was suppressed, reflecting the inhibitory effect of $p21^{Cip1}$ on cell cycle progression. Additionally, lymphocyte infiltration, expression of inflammatory cytokines, and destruction of the bone and cartilage were inhibited. To determine why the cell cycle regulator gene exerted such anti-inflammatory effects, we investigated gene expression by rheumatoid synovial fibroblasts with or without the $p21^{Cip1}$ gene transferred. We have found that $p21^{Cip1}$ gene transfer down-regulates expression of various inflammatory mediators and tissue-degrading proteinases that are critically involved in the pathology of rheumatoid arthritis. These molecules included IL-6, -8, type I IL-1R (IL-1R1), monocyte chemoattractant protein-1, macrophage inflammatory protein-3α, cathepsins B and K, and matrix metalloproteinases-1 and -3. Down-regulation of IL-1R1 by $p21^{Cip1}$ resulted in attenuated responsiveness to IL-1. Inhibition of the inflammatory gene expression by $p21^{Cip1}$ was seen even when IL-1 is absent. This IL-1R1-independent suppression was accompanied by reduced activity of c-Jun N-terminal kinase, which was associated with $p21^{Cip1}$, and inactivation of NF-κB and AP-1. These multiple regulatory effects should work in concert with the primary effect of inhibiting cell cycle in ameliorating the arthritis, and suggest a heretofore unexplored relationship between cyclin-dependent kinase inhibitor gene and inflammatory molecules. ***The Journal of Immunology*, 2003, 171: 4913–4919.**

Synovial tissue from healthy individuals consists of a single layer of synovial cells without infiltration of inflammatory cells. In rheumatoid synovial tissue, lymphocytes and macrophages are recruited and activated, and these activated macrophages release high concentrations of inflammatory cytokines. In response to these cytokines, synovial fibroblasts proliferate vigorously and form villous hyperplastic synovial tissues. These fibroblasts secrete inflammatory mediators, which further attract inflammatory cells and stimulate growth of the synovial fibroblasts as well as that of vascular endothelial cells (1). These activated macrophages and fibroblasts produce tissue-degrading proteinases (2). Thus, the invasive hyperplastic synovial tissue, termed pannus, is directly responsible for structural and functional damage of the affected joints.

Therapeutic intervention against rheumatoid arthritis (RA)[3] could be aimed at any one of these steps. Recently developed biological reagents that block activities of TNF-α have proved to be beneficial in clinical settings. However, they and other conventional drugs do not necessarily control synovial inflammation and hyperplasia in all patients. We hypothesized that the proliferation of the synovial fibroblasts is a common outcome of the multiple inflammatory processes in RA. If synovial fibroblasts become refractory to the proliferative stimuli, the tissue-degrading pannus should not develop. This idea led us to explore new therapeutic approaches that directly control synovial cell proliferation (3–5). The molecules we have focused on are cyclin-dependent kinase inhibitors (CDKIs). These intracellular proteins inhibit kinase activity of cyclin/cyclin-dependent kinase (CDK) complexes that are required for cell cycle progression (6).

Our previous studies have shown that CDKIs $p16^{INK4a}$ and $p21^{Cip1}$ are not expressed in vivo in the rheumatoid synovial tissues, but readily induced in vitro in cultured rheumatoid synovial fibroblasts (RSF). Induction of $p16^{INK4a}$ is characteristic of RSF (3). In vitro inducibility of $p16^{INK4a}$ and $p21^{Cip1}$ suggested to us that their induction in vivo in the rheumatoid joints could be an ideal approach to suppression of the proliferative synovitis. This was substantiated by intraarticular transfer of the $p16^{INK4a}$ or $p21^{Cip1}$ gene to rodent models of RA (4, 5). These gene therapies suppressed synovial hyperplasia and also inhibited lymphocyte infiltration and destruction of the bone and cartilage of the treated joints. Expression of inflammatory cytokines such as IL-1, -6 and TNF-α was suppressed even in the small amount of hyperplastic synovial tissues that remained after the gene transfer (4). These data argued that induction of CDKI ameliorated the arthritis not only by inhibition of cell cycle but by other unknown functions that suppressed the inflammatory network in the arthritic joint.

Unlike the other CDKIs, $p21^{Cip1}$ binds to various molecules related to gene expression and exerts differential effects on different cells (7). However, little is known about the effects of $p21^{Cip1}$ on gene expression in the inflamed tissues. We show here that up-regulated expression of the $p21^{Cip1}$ gene in RSF suppresses expression of various inflammatory molecules that play critical roles in the pathology of RA. Manipulation of these multiple

Department of Bioregulatory Medicine and Rheumatology, Graduate School, Tokyo Medical and Dental University, Tokyo, Japan

Received for publication December 30, 2002. Accepted for publication August 20, 2003.

The costs of publication of this article were defrayed in part by the payment of page charges. This article must therefore be hereby marked *advertisement* in accordance with 18 U.S.C. Section 1734 solely to indicate this fact.

[1] This work was supported by grants from the Japanese Ministry of Health, Labor and Welfare, from the Japanese Ministry of Education, Culture, Sports, Science and Technology, Japan, and from the Kato Memorial Bioscience Foundation.

[2] Address correspondence and reprint requests to Dr. Hitoshi Kohsaka, Bioregulatory Medicine and Rheumatology, Graduate School, Tokyo Medical and Dental University, 1-5-45 Yushima, Bunkyo-ku, Tokyo 113-8519, Japan. E-mail address: kohsaka.rheu@tmd.ac.jp

[3] Abbreviations used in this paper: RA, rheumatoid arthritis; CDKI, cyclin-dependent kinase inhibitor; CDK, cyclin/cyclin-dependent kinase; RSF, rheumatoid synovial fibroblast; IL-1ra, IL-1R antagonist; JNK, c-Jun N-terminal kinase; IL-1R1, type I IL-1R; MCP, monocyte chemoattractant protein; MMP, matrix metalloproteinase; MIP, macrophage inflammatory protein; TLR, Toll-like receptor.

0022-1767/03/$02.00

molecular events should contribute to the therapeutic effects of p21^{Cip1} gene therapy.

Materials and Methods

Cell culture and recombinant adenoviruses

Synovial tissues were obtained from patients who had responded poorly to anti-rheumatic drugs and underwent joint replacement or synovectomy for active rheumatoid synovitis at Tokyo Medical and Dental University Hospital (Tokyo, Japan), Tokyo Metropolitan Bokuto, or Fuchu Hospital (Tokyo, Japan). The patients fulfilled the American College of Rheumatology criteria for classification of RA (8). All patients gave their consent for all procedures in the present studies, which were also approved by the ethics committee of Tokyo Medical and Dental University. From villous and congestive synovial tissues, RSF were isolated and cultured as described elsewhere (3). They were used at passages 3–11. RSF were infected with AxCAp21 adenovirus, containing a human p21^{Cip1} gene (5, 9), or Ax1w1 adenovirus (Riken Gene Bank, Saitama, Japan), which lacks insert genes, at 50 multiplicity of infection. Some RSF were stimulated by 5 ng/ml TNF-α (Genzyme, Cambridge, MA), 5 ng/ml IL-1β (PeproTech, Rocky Hill, NJ), and 25 μM indomethacin (Sigma-Aldrich, St. Louis, MO). In preliminary experiments, 5 ng/ml was determined to be the optimal concentration for each cytokine to stimulate RSF. RNeasy kit (Qiagen, Valencia, CA) with DNase I treatment was used to isolate total RNA. For ELISA, the virus-infected RSF were cultured for three days, transferred to microwells at 1.0×10^5 cells/ml, and incubated for 12 h. After replacement of the culture medium, RSF were further cultured for 24 h with 10% serum alone, 5 ng/ml IL-1β together with 25 μM indomethacin, 5 ng/ml TNF-α, a combination of IL-1β, indomethacin, and TNF-α, or 5 μg/ml LPS of *Escherichia coli* O55:B5 (Sigma-Aldrich). One hundred ng/ml IL-1R antagonist (IL-1ra) (R&D Systems, Mckinley, MN), which was sufficient for the inhibition of 10 pg/ml IL-1β, was added to some wells. The culture supernatants were collected after 24 h. For Western blotting, RSF were lyzed for protein extraction at three days after the adenoviral infection (3). To assess transcription factor and c-Jun N-terminal kinase (JNK) activities in RSF that were incubated for 30 min in the medium containing 10% FBS with or without supplementation of 5 μg/ml LPS, nuclear extracts and cell lysates were prepared using Nuclear Extract Kit (Active Motif, Carlsbad, CA) or SAPK/JNK assay kit (Cell Signaling, Beverly, MA). The effects of the p21^{Cip1} gene were studied at three days after the adenoviral infection.

Northern blot analyses

Northern blotting was conducted as described elsewhere (10). Human monocyte chemoattractant protein (MCP)-1 cDNA (No. 65933, American Type Culture Collection, Manassas, VA), human GAPDH cDNA (Life Technologies, Rockville, MD), and PCR products of type I IL-1R (IL-1R1), cathepsins B and K, and matrix metalloproteinases (MMP)-1 and -3 were used as probes. Fragments of IL-1R1, cathepsins B and K, and MMPs-1 and -3 cDNA were generated with RT-PCR using cDNA derived from RSF. PCR was conducted with *Taq* polymerase (Life Technologies) and sets of specific primers: human IL-1R1-specific primers (11), human MMP-1-specific primers (12), human MMP-3-specific primers (12), human cathepsin B-specific primers (5′-TAG GAT CTG GCT TCC AAC AT-3′ (sense) and 5′-CCA CGG CAG ATT AGA TCT TT-3′ (antisense)) and human cathepsin K-specific primers (5′-AAC GAA GCC AGA CAA CAG ATT TCC-3′ (sense), 5′-GAT TTG GCT GGC TGG AGT CAC A-3′ (antisense)). Annealing temperatures were 58°C for IL-1R1, and cathepsins B and K cDNA, and 60°C for MMP-1 and -3 cDNA. The products were purified and labeled with [α-^{32}P]dATP (Amersham Biosciences, Buckinghamshire, UK) and hybridized with the Northern blot membranes. Digital image files were generated with Phosphorimaging Screens and the BAS-2500 PhosphoImager, and analyzed with MacBAS 2.5.2 Software (Fuji Film, Kanagawa, Japan).

Western blot analyses and immunoprecipitation

Rabbit anti-human IL-1R1 Abs, rabbit anti-human Toll-like receptor (TLR)-4 Abs, and rabbit anti-human p21^{Cip1} Abs (sc-688, sc-10741 and sc-387, respectively, Santa Cruz Biotechnology, Santa Cruz, CA) were used as primary Abs for Western blot analyses. HRP-conjugated anti-rabbit IgG polyclonal Abs (NA-934, Amersham Biosciences) were used as the secondary Abs. Bound Abs were visualized with ECL or ECL-plus (Amersham Biosciences). Signal intensities were quantified with NIH Image ver. 1.62 (National Institutes of Health, Bethesda, MD). JNKs 1–3 were immunoprecipitated using mouse anti-human JNK2 Ab (sc-7345, Santa Cruz Biotechnology) (13).

ELISA

ELISA kits for IL-1β, IL-6, IL-8, MCP-1, TNF-α (BioSource International, Camarillo, CA), IL-1α, macrophage inflammatory protein (MIP)-3α (R&D Systems), MMP-1 (Amersham Biosciences) and MMP-3 (Fuji Chemical, Toyama, Japan) were used to quantify the protein levels in the culture supernatants.

Multiwell colorimetric transcription factor assays and JNK kinase assay

Using Trans AM AP-1/c-Jun, NF-κBp50, and p65 Transcription Factor Assay Kits (Active Motif), the nuclear extracts of RSF were examined for DNA binding activities of AP-1 and NF-κB (14). SAPK/JNK Assay Kit (Cell Signaling) was used to examine whole cell lysates for their JNK kinase activities to phosphorylate c-Jun substrates. The amount of the c-Jun substrate was standardized by immunoblotting with anti c-Jun Ab (sc-44, Santa Cruz Biotechnology).

Statistics

Signal intensity ratios of Northern and Western blot analyses, and protein concentrations were compared with a paired Student's *t* test using StatView-5.0J software (SAS Institute, Cary, NC).

Results

p21^{Cip1} suppresses IL-1R1 and IL-6 expression by RSF

RSF samples derived from rheumatoid joints were cultured in vitro. Expression of p21^{Cip1} was not detected in any of the samples. They were infected with the AxCAp21 adenoviruses or the Ax1w1 adenoviruses. At three days postinfection, when the AxCAp21-infected RSF express p21^{Cip1} at the highest level, the cells were harvested for RNA and protein extraction.

In preliminary experiments using a few RSF samples and commercial DNA array systems, MCP-1, IL-1R1, and cathepsins B and K genes, which are related to RA pathology, showed a tendency to be down-regulated by the p21^{Cip1} gene transfer. Indeed, Northern blot analysis revealed that the IL-1R1 mRNA expression was significantly reduced in RSF overexpressing p21^{Cip1}, compared with those infected with the control adenoviruses (Fig. 1*A*). Reflecting this, Western blot analyses of the total cell lysates showed that the IL-1R1 protein expression was reduced in the RSF expressing p21^{Cip1} (Fig. 1*B*).

The DNA array analyses suggested no differential expression of IL-6 in the unstimulated RSF. However, when RSF were stimulated by TNF-α and IL-1β before the DNA array analysis, IL-6, as well as IL-8, MCP-1, MIP-3α, MMP-1, MMP-3, and cathepsin K genes showed a tendency to be down regulated by p21^{Cip1}. This was consistent with the fact that TNF-α and IL-1, both of which are critically involved in activating RSF in the rheumatoid joints, stimulate RSF to promote secretion of various cytokines including IL-6 (15). The unstimulated RSF did not release IL-1α, IL-1β, or TNF-α above the lowest limit of detection in the ELISA (3.9 pg/ml). These facts implied that the suppression of IL-6 in the stimulated RSF could be attributable to the down-regulation of IL-1R1. To address this issue, RSF were stimulated independently with IL-1β, TNF-α, or a combination of the two. The culture supernatants were examined for the IL-6 concentration with ELISA. Each stimulation promoted IL-6 production. The effects of IL-1β were suppressed significantly by p21^{Cip1} while the effects of TNF-α were not attenuated (Fig. 1*C*). Effects of the adenoviral infection alone on the IL-6 secretion were minimal (Fig. 1*D*). Thus, the down-regulation of IL-1R1 was biologically relevant to the suppression of IL-6.

To determine whether other pathways that regulate IL-6 production are affected, RSF were stimulated with LPS. Western blot analysis confirmed that Toll-like receptor (TLR)4, which is a receptor for LPS, was not down-regulated by p21^{Cip1} (Fig. 1*E*). Nevertheless, the p21^{Cip1} expression suppressed the IL-6 production

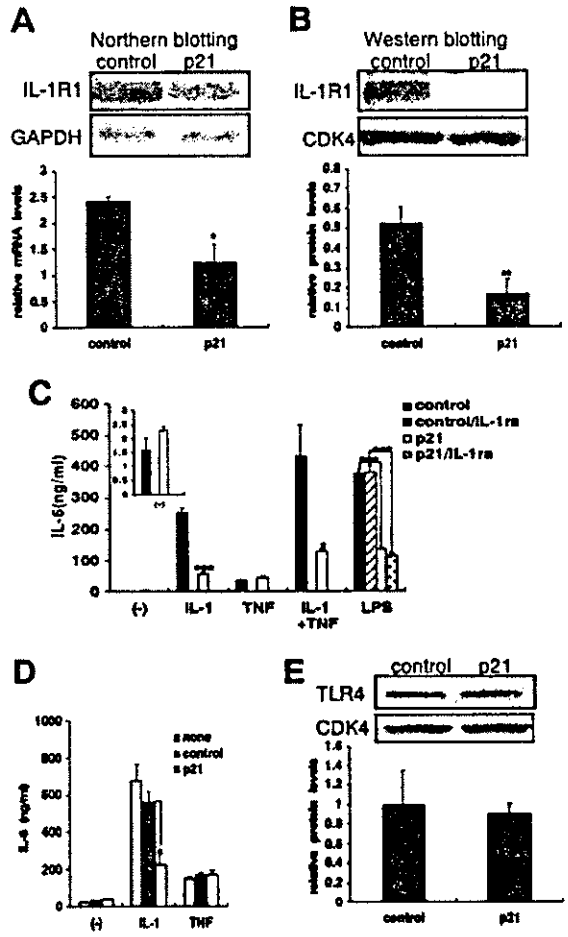

FIGURE 1. Suppression of inflammatory cytokine and cytokine receptor expression by $p21^{Cipl}$. *A*, RNA from the $p21^{Cipl}$ adenovirus-infected (p21) and control adenovirus-infected RSF (control) were examined for IL-1R1 and GAPDH mRNA expression by Northern blot analysis. Representative blots of one of three samples are shown in the upper panel. Signal intensities of IL-1R1 were normalized with those of GAPDH (relative mRNA levels), and are shown in the lower panel. The columns and bars represent the mean and SD of three samples. Mean reduction by $p21^{Cipl}$ was 48.2%. Statistical evaluation was conducted by paired Student's *t* test. *, $p < 0.05$. *B*, The cells from the same donor were examined for IL-1R1 and CDK4 protein expression by Western blot analysis. Representative blots of one of three samples are shown in the *upper panel*. Signal intensities of IL-1R1 protein were normalized with those of constitutively expressed CDK4 (relative protein levels), and are shown in the *lower panel*. Mean reduction of expression by $p21^{Cipl}$ was 67.6%. **, $p < 0.01$. *C*, RSF infected with the $p21^{Cipl}$ adenoviruses (open columns), and infected with the control adenoviruses (solid columns) were cultured without stimulation (−) or stimulated with IL-1β (IL-1), TNF-α (TNF), or combination of IL-1β and TNF-α (IL-1+TNF) for 24 h. RSF were stimulated with LPS for 24 h in a separate set of experiments, where some RSF were treated with IL-1ra after the infection with the control adenoviruses (hatched column) or with the p21 adenoviruses (dotted column). IL-6 in the culture supernatants was measured by ELISA. Representative data of three independent experiments are shown. Columns and bars show the mean and SD of triplicate cultures. Mean reduction of expression by $p21^{Cipl}$ in IL-1, IL-1+TNF, LPS, and LPS+IL-1ra were 77.4, 64.3, 69.4, and 64.3%, respectively. *, $p < 0.05$ and ***, $p < 0.005$. *D*, RSF infected with the $p21^{Cipl}$ adenoviruses (open columns), and infected with the control adenoviruses (solid columns) and noninfected RSF (gray column) were cultured without stimulation (−) or stimulated with IL-1β (IL-1) or TNF-α (TNF) for 24 h. IL-6 in the culture supernatants was measured by ELISA. Representative data of two experiments are shown. Columns and bars show the mean and SD of triplicate cultures. No statistical differences were found between IL-6 production by control-virus infected RSF and that by noninfected RSF. *E*, Expression of TLR4 and CDK4 proteins was analyzed by Western blot analysis. Representative blots of one of three samples are shown. The relative protein levels of TLR4 to CDK4 are shown as columns and bars. TLR4 protein level was not suppressed by $p21^{Cipl}$.

that was induced by LPS (Fig. 1*C*). Again, the culture supernatants of the LPS-stimulated RSF did not contain detectable amounts of IL-1 (<3.9 pg/ml) or TNF-α (<1.7 pg/ml). To eliminate the effect of a trace amount of IL-1 that might possibly have been secreted with the LPS stimulation, 100 ng/ml IL-1ra, a competitive inhibitor of IL-1α and IL-1β, was added to the culture. This treatment did not alter the results whereas the same concentration of IL-1ra suppressed the IL-6 production by RSF that were stimulated with 10 pg/ml IL-1β (data not shown).

$p21^{Cip1}$ suppresses inflammatory chemokine expression by RSF

The $p21^{Cipl}$-induced reduction of the MCP-1 mRNA expression by unstimulated RSF was elucidated by Northern blot analyses (Fig. 2*A*). This was reflected in the reduced MCP-1 concentration in the culture supernatants of the $p21^{Cipl}$-expressing RSF. As was the case in the IL-6 expression, addition of IL-1ra did not alter the results (Fig. 2*B*).

ELISA of MCP-1 in the culture supernatants of RSF stimulated with IL-1β and TNF-α validated the stimulatory effects of these cytokines, and also suppression by $p21^{Cipl}$ (Fig. 2*C*). The effect of IL-1β was significantly suppressed by the $p21^{Cipl}$expression, while that of TNF-α was unchanged (Fig. 2*C*). These results confirmed the biological significance of the IL-1R1 down-regulation. Furthermore, LPS stimulated RSF to increase MCP-1 production. This was suppressed by $p21^{Cipl}$. Addition of IL-1ra did not attenuate the LPS-induced production of MCP-1. Thus, the suppression in this setting was also independent of IL-1 (Fig. 2*C*).

In accordance with the results of the preliminary DNA array analysis, MIP-3α or IL-8 protein levels were suppressed by $p21^{Cipl}$ in the culture supernatants of RSF only when they were stimulated with IL-1β and TNF-α. The effect of IL-1β was significantly reduced by the $p21^{Cipl}$ expression, while that of TNF-α was unchanged. LPS also stimulated MIP-3α production. This IL-1-independent effect was partially inhibited by $p21^{Cipl}$. Similarly, the production of IL-8 was increased both by IL-1β and TNF-α. The effect of IL-1β but not that of TNF-α was inhibited by $p21^{Cipl}$. LPS exerted a stimulatory effect on IL-8 production comparable to that of TNF-α, which was inhibited significantly by $p21^{Cipl}$.

$p21^{Cip1}$ suppresses expression of tissue-degrading proteinases

Northern blot analyses confirmed that $p21^{Cipl}$ suppresses expression of cathepsins B and K in the unstimulated RSF, and that of MMP-1 and -3 in the stimulated RSF (Fig. 3, *A–D*).

These changes were reproduced when the concentrations of MMP-1 and -3 in the culture supernatants were determined (Fig. 3, *E* and *F*). Neither MMP was detected in the supernatants of the unstimulated RSF. MMP-1 production was increased by IL-1β and TNF-α. The combination of these two cytokines had a synergistic effect. The effects of IL-1 were significantly suppressed by $p21^{Cipl}$. As was the case in the cytokine production, LPS increased production of MMP-1. This effect was partially suppressed by $p21^{Cipl}$. The production MMP-3 was increased by IL-1β and LPS. TNF-α alone had no apparent effect but showed a synergistic effect with IL-1β. Again, the effect of IL-1β was suppressed by $p21^{Cipl}$, and the effect of LPS was abrogated completely by $p21^{Cipl}$.

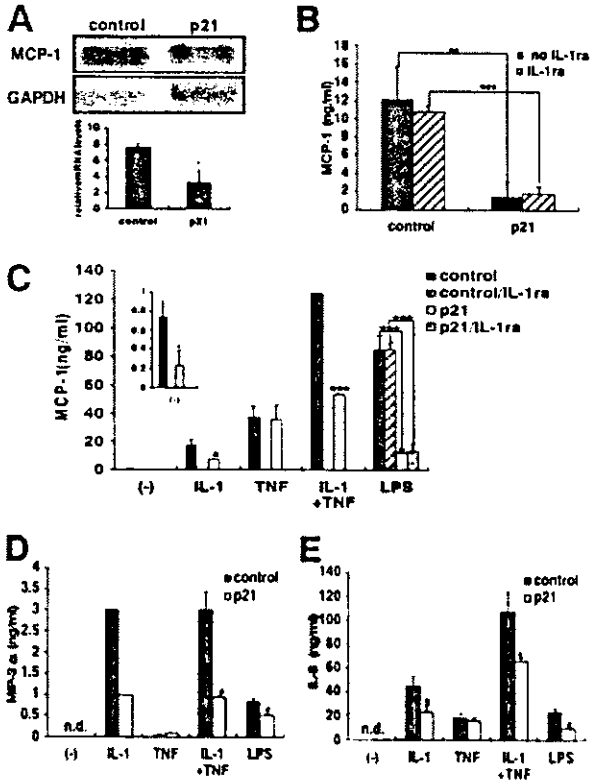

FIGURE 2. Suppression of inflammatory chemokine expression by p21^{Cip1}. *A*, The AxCAp21 adenovirus-infected (p21) and control adenovirus-infected (control) RSF from three RA patients were examined for MCP-1 mRNA expression by Northern blot analysis. RSF were not stimulated with cytokines. Representative results of one of three samples are shown in the *upper panel*. Signal intensities of MCP-1 messages normalized with those of GAPDH messages (relative mRNA levels) are shown as columns and bars, representing the mean and SD. Mean reduction of expression by p21^{Cip1} was 57.0%. *, $p < 0.05$. *B*, RSF with or without p21^{Cip1} expression (p21 and control) were cultured without cytokine stimulation. The culture medium was supplemented with FBS alone (solid columns) or with FBS plus IL-1ra (hatched columns). MCP-1 in the culture supernatants was measured by ELISA. Representative data of two experiments are shown. Columns and bars show the mean and SD of triplicate cultures. Mean reduction of expression by p21^{Cip1} was 83.8% (no IL-1ra) and 87.1% (IL-1ra). **, $p < 0.01$ and ***, $p < 0.005$. *C-E*, RSF infected with the p21^{Cip1} adenoviruses (open columns) or control adenoviruses (solid columns) were cultured without stimulation (−) or stimulated with IL-1β (IL-1), TNF-α (TNF), a combination of IL-1β and TNF-α (IL-1+TNF), or LPS for 24 h. Some RSF infected with the control adenoviruses (hatched column), and with the p21 adenoviruses (dotted column) were treated with IL-1ra before LPS stimulation. MCP-1 (C), MIP-3α (D), and IL-8 (E) in the culture supernatants were measured by ELISA. Representative data of two or three experiments are shown. Columns and bars show the mean and SD of triplicate cultures. n. d., not detectable. Mean reduction in expression of MCP-1 by p21^{Cip1} in IL-1, IL-1+TNF, LPS, and LPS + IL-1ra was 58.3, 57.5%, 84.7, and 83.9%, respectively. Mean reduction in expression of IL-8 by p21^{Cip1} in IL-1, IL-1+TNF, and LPS was 48.4, 38.2, and 54.0% and that of MIP-3α was 66.6, 68.7, and 38.7%. *, $p < 0.05$ and ***, $p < 0.005$.

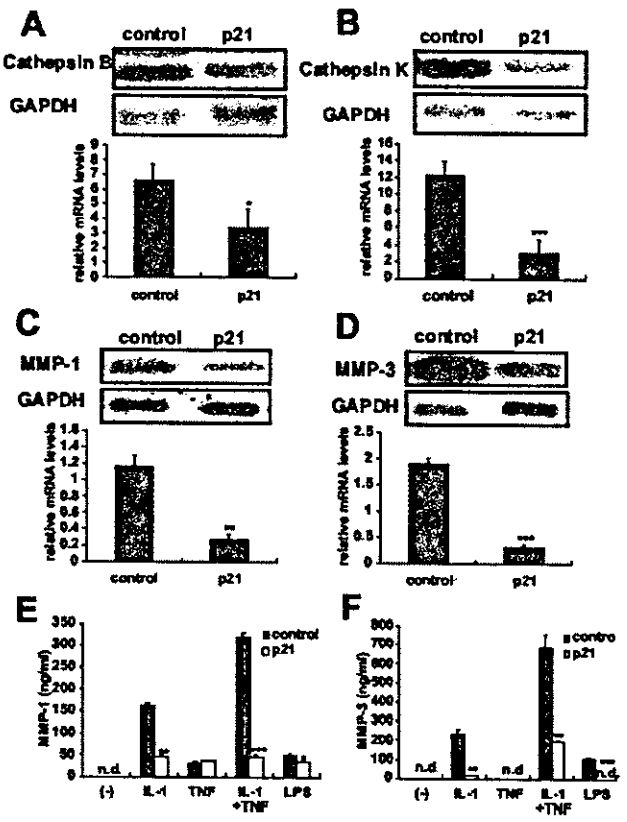

FIGURE 3. Suppression of tissue-degrading proteinase expression by p21^{Cip1}. *A* and *B*, RSF infected with the AxCAp21 adenoviruses (p21) or control adenoviruses (control) were cultured without cytokine stimulation, and examined for cathepsins B (*A*) and K (*B*) mRNA expression by Northern blot analysis. Representative blots are shown in the *upper panels*. Northern blots of cathepsin B showed dual bands representing two transcripts 4.0 and 2.2 kb long (48). The relative levels of mRNA to those of GAPDH mRNA are shown as columns and bars, representing the mean and SD of three samples derived from different patients. Mean reduction in expression of cathepsins B and K by p21^{Cip1} was 47.8 and 75.0%, respectively. *, $p < 0.05$ and ***, $p < 0.005$. *C* and *D*, RSF stimulated with IL-1β and TNF-α were examined for MMP-1 (*C*) and -3 (*D*) mRNA expression by Northern blot analysis. Representative blots of one of three samples are shown in the *upper panels*. The relative levels of mRNA of MMP-1 and -3 are shown as columns and bars, representing the mean and SD of three samples. Mean reduction in expression of MMP-1 and -3 by p21^{Cip1} was 78.6 and 82.6%, respectively. **, $p < 0.01$ and ***, $p < 0.005$. *E* and *F*, RSF infected with the p21^{Cip1} adenoviruses (open columns), and with the control adenoviruses (solid columns) were cultured without stimulation (−) or stimulated with IL-1β (IL-1), TNF-α (TNF), a combination of IL-1β and TNF-α (IL-1+TNF), or LPS for 24 h. MMP-1 and -3 in the culture supernatants were measured by ELISA. Representative data of two experiments are shown. Columns and bars show the mean and SD of triplicate cultures. Unstimulated RSF produced no detectable MMP-1 or -3. Mean reduction in expression of MMP-1 by p21^{Cip1} in IL-1, IL-1+TNF, and LPS was 70.9, 85.3, and 29.5%, respectively, and that of MMP-3 was 92.6, 71.5, and 88.3%, respectively. *, $p < 0.05$; **, $p < 0.01$; ***, $p < 0.005$.

p21^{Cip1} inhibits DNA binding activity of AP-1 and NF-κB

p21^{Cip1} down-regulated expression of MCP-1 and cathepsins B and K in the unstimulated RSF. Although it did not suppress expression of TLR4, it suppressed the LPS-dependent up-regulation of many inflammatory mediators. This has led us to assume that p21^{Cip1} should directly inhibit nonreceptor, intracellular molecules. Since promoter activity of the inflammatory mediator genes that were suppressed by p21^{Cip1} is controlled mostly by NF-κB and AP-1 transcription factors, we investigated the DNA binding activities of these factors in the unstimulated and LPS-stimulated RSF. Multiwell colorimetric assays to quantify DNA binding activity of the transcription factors showed that activity of AP-1 was down-regulated by p21^{Cip1} in the unstimulated RSF. Stimulation

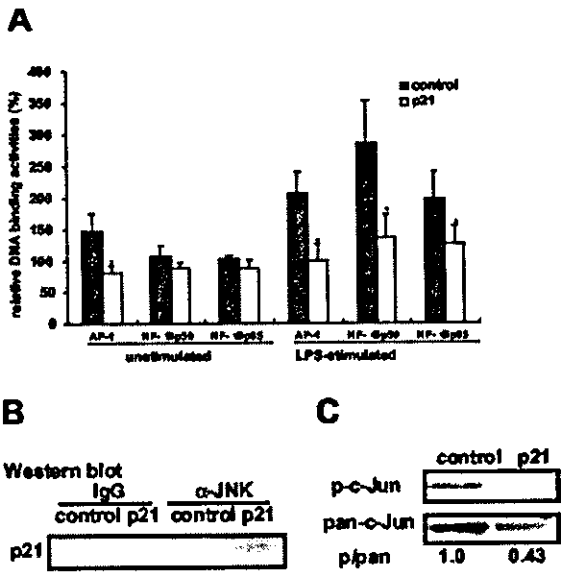

FIGURE 4. Suppression of AP-1 and NF-κB transcription factors by $p21^{Cip1}$. RSF infected with the $p21^{Cip1}$ adenoviruses (p21) or control adenoviruses (control) were cultured with or without LPS stimulation. The DNA binding activities of AP-1 and NF-κB in the adenoviruses-infected RSF relative to those of the uninfected RSF without stimulation are shown (A). Columns and bars show the mean and SD of triplicate cultures. $p21^{Cip1}$ suppressed DNA binding activity of AP-1, but did not suppress that of NF-κBp50 or p65 significantly in the unstimulated RSF. Mean reduction in expression of the AP-1 activity was 47.3%. In the LPS-stimulated RSF, $p21^{Cip1}$ suppressed DNA binding activities of AP-1, NF-κBp50, and p65. Mean reduction in expression of AP-1, NF-κBp50, and NF-κB p65 by $p21^{Cip1}$ was 47.4, 52.6, and 41.3%, respectively. $*, p < 0.05$. $p21^{Cip1}$ in the $p21^{Cip1}$-expressing RSF stimulated with LPS (p21) was coimmunoprecipitated with anti-JNK Ab (α-JNK), but not with control IgG (IgG). No precipitation was found when RSF were infected with the control viruses (control) (*B*). Phosphorylation of c-Jun (p-c-Jun) was suppressed in RSF infected with the $p21^{Cip1}$ viruses (p21) but not in RSF infected with the control viruses (control). Reduction in expression of relative p-c-Jun levels to whole c-Jun (pan-c-Jun) was 57% (*C*). The results are representatives of two independent experiments.

with LPS up-regulated activities of NF-κB p50, p65, and AP-1, all of which were down-regulated by $p21^{Cip1}$ (Fig. 4*A*).

It was shown that $p21^{Cip1}$ associates with JNK in other type of cells, which results in reduction of the JNK enzymatic activity that activates AP-1 (16). Using anti-JNK Ab, we immunoprecipitated JNK in cell lysates of $p21^{Cip1}$-expressing RSF that were stimulated with LPS. Immunoblotting of the precipitants with anti-$p21^{Cip1}$ Abs revealed that $p21^{Cip1}$ indeed associated with JNK (Fig. 4*B*). Phosphorylation of c-Jun substrates showed that kinase activity of JNK was suppressed in the $p21^{Cip1}$-expressing RSF (Fig. 4*C*). Thus, the IL-1R1-independent suppression should be at least partly due to down-regulation of these pathways.

Discussion

Since the primary function of CDKIs is the inhibition of kinase activity of CDKs, the anticipated effect of the $p21^{Cip1}$ expression in RSF was suppression of cell cycle progression. Indeed, RSF infected with the AxCAp21 viruses did not respond in vitro to proliferative stimuli by proinflammatory cytokines or by growth factors (4). In vivo transfer of the $p21^{Cip1}$ gene into the arthritic joints of RA model rats suppressed synovial hyperplasia and cell cycle progression of the synovial fibroblasts (5).

However, the present study has revealed that $p21^{Cip1}$ exerts multiple auxiliary effects: down-regulation of cytokine, chemokine, cytokine receptor, and proteinase expression critically involved in the pathology of RA. We found previously that expression of proinflammatory cytokines such as IL-1, IL-6, and TNF-α was unexpectedly inhibited in vivo in the synovial tissues treated with $p21^{Cip1}$ gene transfer (4). The present report provides molecular evidence showing that $p21^{Cip1}$ expression has a wide array of anti-inflammatory and bone-protective effects. Down-regulation of IL-1R1, and also IL-1R-independent inactivation of intracellular signaling pathways appeared to account for these effects (Fig. 5). Finally, these effects suggest that the $p21^{Cip1}$ gene transfer might ameliorate types of inflammatory arthritides other than RA.

The down-regulation of IL-6 observed in vivo was actually seen in vitro in $p21^{Cip1}$-expressing RSF while the expression of IL-1 or TNF-α were not significantly modulated. It is possible that the decreased expression of IL-1 and TNF-α in the synovial tissues was due to their down-regulation in the synovial macrophages. The macrophages are the primary source of these cytokines and, together with synovial fibroblasts, were targeted by the intraarticular adenoviral gene transfer (15, 17). Alternatively, the down-regulation of IL-1 and TNF-α might result from en bloc suppression of the inflammatory cytokine/chemokine network, multiple members of which were suppressed by $p21^{Cip1}$.

IL-6, in the rheumatoid synovial tissues, derives from the activated synovial macrophages and fibroblasts, and stimulates local osteoclasts to resorb the bone matrices in the affected joints. It also stimulates T and B lymphocytes. This has made this cytokine the target of a new biological reagent that is currently in clinical trials (18, 19). IL-8 produced by the activated synovial cells contributes to recruitment of neutrophils and T lymphocytes and to neovascularization in the rheumatoid tissues (20). The other chemokines, MCP-1 and MIP-3α, both evoke migration and activation of lymphocytes and macrophages in the rheumatoid synovial tissues (21, 22). Blockage of MCP-1 receptor was effective in treating an animal model of RA (23). Thus, the cytokines and chemokines down-regulated by $p21^{Cip1}$ all play crucial roles in the rheumatoid inflammation.

Tissue degrading enzymes, such as MMPs and cathepsins, are abundantly expressed in rheumatoid synovial tissues. MMP-1 and -3 degrade collagen and proteoglycans that compose the matrices of bone and cartilage. In addition, it has been proposed that MMP-3 cleaves many proMMPs in the initiation of the proteinase cascade in rheumatoid joints (2). Treatment to inhibit MMP-1 production prevented bone destruction in adjuvant arthritis of rats

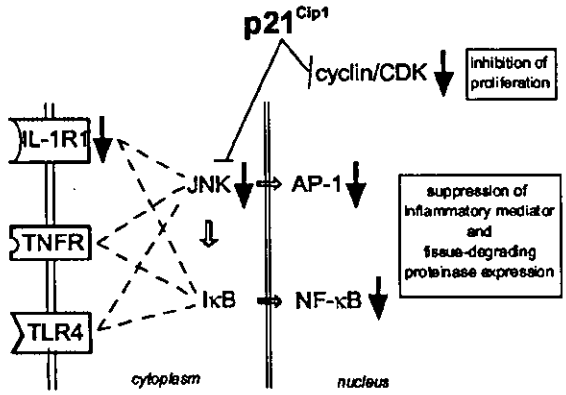

FIGURE 5. Multiple effects of $p21^{Cip1}$ on RSF. $p21^{Cip1}$ inhibited kinase activity of cyclin/CDK complexes, and down-regulated IL-1R1 expression and DNA binding activities of NF-κB and AP-1. These effects were mediated at least by binding of $p21^{Cip1}$ to cyclin/CDK complexes and JNK, and resulted in inhibition of proliferation and in suppression of IL-6, -8, MCP-1, MIP-3α, cathepsins B and K, and MMP-1 and -3 expression.

(24). Cathepsin B might contribute to rheumatoid joint damage by degrading collagen (25, 26, 27). Cathepsin K is not only expressed by osteoclasts, but also by synovial fibroblasts, contributing to bone destruction in the rheumatoid joints (28, 29). Down-regulation of these proteinases in the $p21^{Cip1}$-expressing RSF was consistent with the remarkable inhibition of bone and cartilage degeneration observed in the $p21^{Cip1}$ gene therapy.

Expression of IL-1R1 was suppressed by $p21^{Cip1}$. IL-1 is one of the critical cytokines in the rheumatoid inflammation. It enhances migration of inflammatory cells into the synovial tissues and stimulates production of cytokines, chemokines and MMPs (15). Its blockade by an antagonist ameliorates RA (30–32). We saw that IL-1-triggered promotion of IL-6, IL-8, MCP-1, MIP-3α, and MMP-1 and -3 release from RSF was significantly suppressed by $p21^{Cip1}$. These results argue that down-regulation of IL-1R1 must be functionally relevant to the therapeutic effects.

MCP-1 and cathepsin B and K expression was suppressed even when RSF were not stimulated. Conventional ELISA detected no IL-1 in the culture supernatant of the unstimulated RSF. The blockade of IL-1 with IL-1ra did not affect the results. Thus, the suppression observed in the unstimulated RSF was not mediated by the down-regulation of IL-1R1. LPS also up-regulated MCP-1 expression, and induced expression of IL-6, IL-8, MIP-3α, and MMP-1 and -3. This was not accompanied by reduced expression of TLR4, which is a signaling receptor for LPS. The LPS-stimulated RSF under these conditions did not release a detectable level of IL-1 into the culture supernatants, and IL-1 blockade by IL-1ra did not alter the results. Thus, inhibition of the inflammatory molecule expression could be at least partly due to modulation of intracellular pathways that are independent of IL-1R1. IL-1 and TNF-α have distinct pathways in the afferent arm of the signal transduction whereas IL-1 and LPS share a part of the signal transduction molecules (33). Presumably, this difference should account for the distinct effect of $p21^{Cip1}$ on TNF-α and LPS stimulation.

The IL-1R-independent suppression was accompanied by reduced activity of NF-κB and AP-1. In the rheumatoid synovial tissues these factors activate transcription of various inflammatory cytokines, chemokines, and proteinases including those analyzed in the present studies (17, 24, 34–42). In agreement with our observation, constitutive expression of MCP-1 by mesangial cells required activation of AP-1 (43). Notably, the promoter of the *IL-1R1* gene has two AP-1-like binding sites (44). This suggests that the repressed activity of AP-1 might contribute to the down-regulation of IL-1R1.

Depending on the cell type, $p21^{Cip1}$ binds to a variety of intracellular proteins other than CDKs. These include signal transduction molecules and transcription factors (7). We have shown that $p21^{Cip1}$ indeed binds to JNK and suppresses its kinase activity in RSF. It is known that JNK could activate NF-κB by degrading Iκ-B (45, 46). Thus, interaction of $p21^{Cip1}$ with mitogen-activated protein kinase might account for the reduced activity of AP-1 and NF-κB.

Chang et al. (47) used the DNA array technique to study effects of $p21^{Cip1}$ on gene expression in HT1080 human sarcoma cell line; they observed that genes related to senescence or age-related diseases were induced. We have shown here that $p21^{Cip1}$ expression modulates the expression of genes related to inflammation. Although, Chang et al. found up-regulation of the *cathepsin B* gene in HT1080 cells, the same gene was down-regulated in RSF. It is probable that the effects of $p21^{Cip1}$ depend on the cell types.

In conclusions, $p21^{Cip1}$ gene transfer to the RSF regulated expression of various genes. Its effects include down-regulation of cytokine, chemokine, cytokine receptor and proteinase expression. Down-regulation of IL-1R1, as well as inactivation of intracellular signaling pathways appeared to account for these effects. These collateral effects observed in the $p21^{Cip1}$ gene transfer suggest new links between CDKIs and immunological effector molecules.

Acknowledgments

We thank Drs. T. Muneta, Y. Kuga, and J. Hasegawa for providing synovial samples; Drs. N. Terada and M. Ikeda for providing adenoviruses; Drs. R. Koike, H. Hagiyama, T. Nanki, and H. Nishitoh for their technical support and advice; and also Dr. N. Nishimura at Genetic Laboratory (Sapporo, Japan) performing DNA array experiments. We are grateful to Dr. T. Page for reviewing the manuscript.

References

1. Hale, L., and B. Haynes. 1997. Pathology of rheumatoid arthritis and associated disorders. In *Arthritis and Allied Conditions: A Textbook of Rheumatology.* W. Koopman, ed. Williams & Wilkins, Baltimore, p. 993.
2. Okada, Y. 2001. Proteinases and matrix degradation. In *Kelly's Textbook of Rheumatology.* Vol. 1. S. Ruddy, E. D. Harris, Jr., C. B. Sledge, eds. W. B. Saunders, Philadelphia, p. 55.
3. Taniguchi, K., H. Kohsaka, N. Inoue, Y. Terada, H. Ito, K. Hirokawa, and N. Miyasaka. 1999. Induction of the $p16^{INK4a}$ senescence gene as a new therapeutic strategy for the treatment of rheumatoid arthritis. *Nat. Med. 5:760.*
4. Nasu, K., H. Kohsaka, Y. Nonomura, Y. Terada, H. Ito, K. Hirokawa, and N. Miyasaka. 2000. Adenoviral transfer of cyclin-dependent kinase inhibitor genes suppresses collagen-induced arthritis in mice. *J. Immunol. 165:7246.*
5. Nonomura, Y., H. Kohsaka, K. Nasu, Y. Terada, M. Ikeda, and N. Miyasaka. 2001. Suppression of arthritis by forced expression of cyclin-dependent kinase inhibitor $p21^{Cip1}$ gene into the joints. *Int. Immunol. 13:723.*
6. Sherr, C. J., and J. M. Roberts. 1999. CDK inhibitors: positive and negative regulators of G_1-phase progression. *Genes Dev. 13:1501.*
7. Dotto, G. P. 2000. $p21^{WAF1/Cip1}$: more than a break to the cell cycle? *Acta Biochim. Biophys. 1471:M43.*
8. Arnett, F. C., S. M. Edworthy, D. A. Bloch, D. J. McShane, J. F. Fries, N. S. Cooper, L. A. Healey, S. R. Kaplan, M. H. Liang, and H. S. Luthra. 1988. The American Rheumatism Association 1987 revised criteria for the classification of rheumatoid arthritis. *Arthritis Rheum. 31:315.*
9. Terada, Y., T. Yamada, O. Nakashima, M. Tamamori, H. Ito, S. Sasaki, and F. Marumo. 1997. Overexpression of cell cycle inhibitors ($p16^{INK4}$ and $p21^{Cip1}$) and cyclin D1 using adenovirus vectors regulates proliferation of rat mesangial cells. *J. Am. Soc. Nephrol. 8:51.*
10. Kumagai, T., T. Miki, M. Kikuchi, T. Fukuda, N. Miyasaka, R. Kamiyama, and S. Hirosawa. 1999. The proto-oncogene Bcl6 inhibits apoptotic cell death in differentiation-induced mouse myogenic cells. *Oncogene 18:467.*
11. Sadouk, M. B., J. P. Pelletier, G. Tardif, K. Kiansa, J. M. Cloutier, and J. Martel-Pelletier. 1995. Human synovial fibroblasts coexpress IL-1R type I and type II mRNA: the increased level of the IL-1 receptor in osteoarthritic cells is related to an increased level of the type I receptor. *Lab. Invest. 73:347.*
12. Moore, B. A., S. Aznavoorian, J. A. Engler, and L. J. Windsor. 2000. Induction of collagenase-3 (MMP-13) in rheumatoid arthritis synovial fibroblasts. *Acta Biochim. Biophys. 1502:307.*
13. Patel, R., B. Bartosch, and J. L. Blank. 1998. $p21^{WAF1}$ is dynamically associated with JNK in human T lymphocytes during cell cycle progression. *J. Cell Sci. 111:2247.*
14. Renard, P., I. Ernest, A. Houbion, M. Art, H. Le Calvez, M. Raes, and J. Remacle. 2001. Development of a sensitive multi-well colorimetric assay for active NF-κB. *Nucleic Acids Res. 29:E21.*
15. Feldmann, M., F. M. Brennan, and R. N. Maini. 1996. Role of cytokines in rheumatoid arthritis. *Annu. Rev. Immunol. 14:397.*
16. Shim, J., H. Lee, J. Park, H. Kim, and E. J. Choi. 1996. A non-enzymatic p21 protein inhibitor of stress-activated protein kinases. *Nature 381:804.*
17. Bondeson, J., B. Foxwell, F. Brennan, and M. Feldmann. 1999. Defining therapeutic targets by using adenovirus: blocking NF-κB inhibits both inflammatory and destructive mechanisms in rheumatoid synovium but spares anti-inflammatory mediators. *Proc. Natl. Acad. Sci. USA 96:5668.*
18. Wendling, D., E. Racadot, and J. Wijdenes. 1993. Treatment of severe rheumatoid arthritis by anti-interleukin-6 monoclonal antibody. *J. Rheumatol. 20:259.*
19. Yoshizaki, K., N. Nishimoto, M. Mihara, and T. Kishimoto. 1998. Therapy of rheumatoid arthritis by blocking IL-6 signal transduction with a humanized anti-IL-6 receptor antibody. *Springer Semin. Immunopathol. 20:247.*
20. Koch, A. E., M. V. Volin, J. M. Woods, S. L. Kunkel, M. A. Connors, L. A. Harlow, D. C. Woodruff, M. D. Burdick, and R. M. Strieter. 2001. Regulation of angiogenesis by the C-X-C chemokines interleukin-8 and epithelial neutrophil activating peptide 78 in the rheumatoid joint. *Arthritis Rheum. 44:31.*
21. Koch, A. E., S. L. Kunkel, L. A. Harlow, B. Johnson, H. L. Evanoff, G. K. Haines, M. D. Burdick, R. M. Pope, and R. M. Strieter. 1992. Enhanced production of monocyte chemoattractant protein-1 in rheumatoid arthritis. *J. Clin. Invest. 90:772.*
22. Chabaud, M., G. Page, and P. Miossec. 2001. Enhancing effect of IL-1, IL-17, and TNF-α on macrophage inflammatory protein-3α production in rheumatoid arthritis: regulation by soluble receptors and Th2 cytokines. *J. Immunol. 167:6015.*
23. Gong, J. H., L. G. Ratkay, J. D. Waterfield, and I. Clark-Lewis. 1997. An antagonist of monocyte chemoattractant protein 1 (MCP-1) inhibits arthritis in the MRL-lpr mouse model. *J. Exp. Med. 186:131.*

24. Han, Z., D. L. Boyle, L. Chang, B. Bennett, M. Karin, L. Yang, A. M. Manning, and G. S. Firestein. 2001. c-Jun N-terminal kinase is required for metalloproteinase expression and joint destruction in inflammatory arthritis. *J. Clin. Invest. 108:73.*
25. Trabandt, A., R. E. Gay, H. G. Fassbender, and S. Gay. 1991. Cathepsin B in synovial cells at the site of joint destruction in rheumatoid arthritis. *Arthritis Rheum. 34:1444.*
26. Cunnane, G., O. FitzGerald, K. M. Hummel, R. E. Gay, S. Gay, and B. Bresnihan. 1999. Collagenase, cathepsin B and cathepsin L gene expression in the synovial membrane of patients with early inflammatory arthritis. *Rheumatology (Oxford) 38:34.*
27. Turk, B., D. Turk, and V. Turk. 2000. Lysosomal cysteine proteases: more than scavengers. *Acta Biochim. Biophys. 1477:98.*
28. Kaneko, M., T. Tomita, T. Nakase, Y. Ohsawa, H. Seki, E. Takeuchi, H. Takano, K. Shi, K. Takahi, E. Kominami, et al. 2001. Expression of proteinases and inflammatory cytokines in subchondral bone regions in the destructive joint of rheumatoid arthritis. *Rheumatology (Oxford) 40:247.*
29. Hou, W. S., W. Li, G. Keyszer, E. Weber, R. Levy, M. J. Klein, E. M. Gravallese, S. R. Goldring, and D. Bromme. 2002. Comparison of cathepsins K and S expression within the rheumatoid and osteoarthritic synovium. *Arthritis Rheum. 46:663.*
30. Dayer, J. M., U. Feige, C. K. Edwards III, and D. Burger. 2001. Anti-interleukin-1 therapy in rheumatic diseases. *Curr. Opin. Rheumatol. 13:170.*
31. Bresnihan, B., J. M. Alvaro-Gracia, M. Cobby, M. Doherty, Z. Domljan, P. Emery, G. Nuki, K. Pavelka, R. Rau, B. Rozman, et al. 1998. Treatment of rheumatoid arthritis with recombinant human interleukin-1 receptor antagonist. *Arthritis Rheum. 41:2196.*
32. Jiang, Y., H. K. Genant, I. Watt, M. Cobby, B. Bresnihan, R. Aitchison, and D. McCabe. 2000. A multicenter, double-blind, dose-ranging, randomized, placebo-controlled study of recombinant human IL-1 receptor antagonist in patients with rheumatoid arthritis: radiologic progression and correlation of Genant and Larsen scores. *Arthritis Rheum. 43:1001.*
33. Beutler, B. 2000. Tlr4: central component of the sole mammalian LPS sensor. *Curr. Opin. Immunol. 12:20.*
34. Fujisawa, K., H. Aono, T. Hasunuma, K. Yamamoto, S. Mita, and K. Nishioka. 1996. Activation of transcription factor NF-κB in human synovial cells in response to TNF-α. *Arthritis Rheum. 39:197.*
35. Asahara, H., K. Fujisawa, T. Kobata, T. Hasunuma, T. Maeda, M. Asanuma, N. Ogawa, H. Inoue, T. Sumida, and K. Nishioka. 1997. Direct evidence of high DNA binding activity of transcription factor AP-1 in rheumatoid arthritis synovium. *Arthritis Rheum. 40:912.*
36. Han, Z., D. L. Boyle, A. M. Manning, and G. S. Firestein. 1998. AP-1 and NF-κB regulation in rheumatoid arthritis and murine collagen-induced arthritis. *Autoimmunity 28:197.*
37. Aupperle, K. R., B. L. Bennett, D. L. Boyle, P. P. Tak, A. M. Manning, and G. S. Firestein. 1999. NF-κB regulation by IκB kinase in primary fibroblast-like synoviocytes. *J. Immunol. 163:427.*
38. Georganas, C., H. Liu, H. Perlman, A. Hoffmann, B. Thimmapaya, and R. M. Pope. 2000. Regulation of IL-6 and IL-8 expression in rheumatoid arthritis synovial fibroblasts: the dominant role for NF-κB but not C/EBPβ or c-Jun. *J. Immunol. 165:7199.*
39. Mengshol, J. A., K. S. Mix, and C. E. Brinckerhoff. 2002. Matrix metalloproteinases as therapeutic targets in arthritic diseases: bull's-eye or missing the mark? *Arthritis Rheum. 46:13.*
40. Auron, P. E., and A. C. Webb. 1994. Interleukin-1: a gene expression system regulated at multiple levels. *Eur. Cytokine Netw. 5:573.*
41. Roebuck, K. A. 1999. Regulation of interleukin-8 gene expression. *J. Interferon Cytokine Res. 19:429.*
42. Gelb, B. D., G. P. Shi, M. Heller, S. Weremowicz, C. Morton, R. J. Desnick, and H. A. Chapman. 1997. Structure and chromosomal assignment of the human cathepsin K gene. *Genomics 41:258.*
43. Lucio-Cazana, J., K. Nakayama, Q. Xu, T. Konta, V. Moreno-Manzano, A. Furusu, and M. Kitamura. 2001. Suppression of constitutive but not IL-1β-inducible expression of monocyte chemoattractant protein-1 in mesangial cells by retinoic acids: intervention in the AP-1 pathway. *J. Am. Soc. Nephrol. 12:688.*
44. Ye, K., C. A. Dinarello, and B. D. Clark. 1993. Identification of the promoter region of human interleukin-1 type I receptor gene: multiple initiation sites, high G+C content, and constitutive expression. *Proc. Natl. Acad. Sci. USA 90:2295.*
45. Spiegelman, V. S., P. Stavropoulos, E. Latres, M. Pagano, Z. Ronai, T. J. Slaga, and S. Y. Fuchs. 2001. Induction of β-transducin repeat-containing protein by JNK signaling and its role in the activation of NF-κB. *J. Biol. Chem. 276:27152.*
46. Das, K. C. 2001. c-Jun NH_2-terminal kinase-mediated redox-dependent degradation of IκB: role of thioredoxin in NF-κB activation. *J. Biol. Chem. 276:4662.*
47. Chang, B. D., K. Watanabe, E. V. Broude, J. Fang, J. C. Poole, T. V. Kalinichenko, and I. B. Roninson. 2000. Effects of $p21^{Waf1/Cip1/Sdi1}$ on cellular gene expression: implications for carcinogenesis, senescence, and age-related diseases. *Proc. Natl. Acad. Sci. USA 97:4291.*
48. DiPaolo, B. R., R. J. Pignolo, and V. J. Cristofalo. 1992. Overexpression of the two-chain form of cathepsin B in senescent WI-38 cells. *Exp. Cell Res. 201:500.*

GITR Activation Induces an Opposite Effect on Alloreactive CD4$^+$ and CD8$^+$ T Cells in Graft-Versus-Host Disease

Stephanie J. Muriglan,[1] Teresa Ramirez-Montagut,[1] Onder Alpdogan,[1] Thomas W. van Huystee,[1] Jeffrey M. Eng,[1] Vanessa M. Hubbard,[1] Adam A. Kochman,[1] Kartono H. Tjoe,[1] Carlo Riccardi,[3] Pier Paolo Pandolfi,[2] Shimon Sakaguchi,[4,5] Alan N. Houghton,[1] and Marcel R.M. van den Brink[1]

[1]*Department of Medicine and Immunology and* [2]*Department of Pathology, Memorial Sloan-Kettering Cancer, New York, NY 10021*

[3]*Department of Clinical and Experimental Medicine, Perugia University Medical School, 06100 Perugia, Italy*

[4]*Department of Experimental Pathology, Institute for Frontier Medical Sciences, Kyoto University, Kyoto 606-8507, Japan*

[5]*Laboratory for Immunopathology, Institute of Physical and Chemical Research, Research Center for Allergy and Immunology, Yokohama 230-0045, Japan*

Abstract

Glucocorticoid-induced tumor necrosis factor receptor family-related gene (GITR) is a member of the tumor necrosis factor receptor (TNFR) family that is expressed at low levels on unstimulated T cells, B cells, and macrophages. Upon activation, CD4$^+$ and CD8$^+$ T cells up-regulate GITR expression, whereas immunoregulatory T cells constitutively express high levels of GITR. Here, we show that GITR may regulate alloreactive responses during graft-versus-host disease (GVHD) after allogeneic bone marrow transplantation (BMT). Using a BMT model with major histocompatibility complex class I and class II disparity, we demonstrate that GITR stimulation in vitro and in vivo enhances alloreactive CD8$^+$CD25$^-$ T cell proliferation, whereas it decreases alloreactive CD4$^+$CD25$^-$ proliferation. Allo-stimulated CD4$^+$CD25$^-$ cells show increased apoptosis upon GITR stimulation that is dependent on the Fas–FasL pathway. Recipients of an allograft containing CD8$^+$CD25$^-$ donor T cells had increased GVHD morbidity and mortality in the presence of GITR-activating antibody (Ab). Conversely, recipients of an allograft with CD4$^+$CD25$^-$ T cells showed a significant decrease in GVHD when treated with a GITR-activating Ab. Our findings indicate that GITR has opposite effects on the regulation of alloreactive CD4$^+$ and CD8$^+$ T cells.

Key words: transplantation immunology • in vivo animal models • immune regulation • lymphocyte activation • T lymphocyte subsets

Introduction

Glucocorticoid-induced tumor necrosis factor receptor family-related gene (GITR), also known as TNFRSF18, is a type I transmembrane protein with high homology to other members of the TNFR family, including 4-1BB, CD27, and OX40 (1, 2). As with other members of the TNFR family, signaling through GITR may induce cell survival or cell death. Stimulation of human and mouse T cells through GITR induces NFκB activation via the TRAF2–NIK signaling pathway (3, 4). The intracellular domain of GITR binds Siva, a cytoplasmic molecule that contains a death domain, and may signal for induction of

S.J. Muriglan and T. Ramirez-Montagut contributed equally to this work.

The online version of this article contains supplemental material.

Address correspondence to Teresa Ramirez-Montagut, Memorial Sloan-Kettering Cancer Center, Kettering 425, Mailbox 111, 1275 York Ave., New York, NY 10021. Phone: (212) 639-5607; Fax: (917) 432-2375; email: ramirezt@mskcc.org

This work was presented at the American Society of Hematology Annual Meeting in 2003, the American Society for Blood and Marrow Transplantation in 2004, the American Association for Cancer Research Annual Meeting in 2004, and the American Association for Immunologists in 2004 in abstract form.

Abbreviations used in this paper: AICD, activation-induced cell death; BMT, BM transplantation; CFSE, carboxyfluorescein succinimidyl ester; GITR, glucocorticoid-induced tumor necrosis factor receptor family-related gene; GITRL, GITR ligand; sGITR, soluble GITR; TCD, T cell–deleted.

 J. Exp. Med. © The Rockefeller University Press • 0022-1007/2004/07/149/9 $8.00
Volume 200, Number 2, July 19, 2004 149–157
http://www.jem.org/cgi/doi/10.1084/jem.20040116